ASTROPHYSICAL S-FACTORS FOR FUSION REACTIONS AND NUCLEOSYNTHESIS

By

VINAY SINGH

Enrollment No. : PHYS04201504002

Variable Energy Cyclotron Centre,
1/AF, Bidhan Nagar, Kolkata-700 064, India

A thesis submitted to the

Board of Studies in Physical Sciences

In partial fulfillment of requirements

for the Degree of

DOCTOR OF PHILOSOPHY

of

HOMI BHABHA NATIONAL INSTITUTE

September, 2019

STATEMENT BY AUTHOR

This dissertation has been submitted in partial fulfillment of requirements for an advanced degree at Homi Bhabha National Institute (HBNI) and is deposited in the Library to be made available to borrowers under rules of the HBNI.

Brief quotations from this dissertation are allowable without special permission, provided that accurate acknowledgement of source is made. Requests for permission for extended quotation from or reproduction of this manuscript in whole or in part may be granted by the Competent Authority of HBNI when in his or her judgment the proposed use of the material is in the interests of scholarship. In all other instances, however, permission must be obtained from the author.

Signature: ___________________

Name of the student: Vinay Singh

DECLARATION

I, hereby declare that the investigation presented in the thesis has been carried out by me. The work is original and has not been submitted earlier as a whole or in part for a degree / diploma at this or any other Institution / University.

Signature: ___________________

Name of the student: Vinay Singh

List of Publications arising from the thesis

Journal

1. "Astrophysical S-factor for deep sub-barrier fusion reactions of light nuclei", Vinay Singh, Debasis Atta, Md. A. Khan, D. N. Basu, *Nucl. Phys A*, **2019**, *986*, 98-106.

2. "Theoretical exploration of S-factors for nuclear reactions of astrophysical importance", Vinay Singh, Joydev Lahiri, D. N. Basu, *Nucl. Phys A*, **2019**, *987*, 260-273.

3. "Big-Bang Nucleosynthesis and primordial lithium abundance problem", Vinay Singh, Joydev Lahiri, Debasis Bhowmick, D. N. Basu, *Journal of Experimental and Theoretical Physics,* **2019,** *128*, 707-712 (English), **2019,** *155*, 832-838 (Russian).

Chapters in books and lectures notes

Conferences

1. "Deep sub-barrier fusion of p+6,7Li, p+D and S-function", Vinay Singh, Debasis Atta, Md. A. Khan, D. N. Basu, *Proceedings of the DAE Symposium on Nuclear Physics*, Bhabha Atomic Research Centre, Mumbai, India, **2018**, *63*, 768-769.

2. "Big-Bang Nucleosynthesis and Lithium abundance", Vinay Singh, Joydev Lahiri, Debasis Bhowmick, D. N. Basu, *Proceedings of the DAE Symposium on Nuclear Physics*, Thapar University, Patiala, Punjab, India, **2017**, *62*, 702-703.

3. "Astrophysical S-factor for sub-barrier Fusion Reaction", Vinay Singh, Debasis Atta, Md. A. Khan, *Proceedings of the DAE Symposium on Nuclear Physics*, Saha Institute of Nuclear Physics, Kolkata, India, **2016**, *61*, 930-931.

Others

Signature

Name of the student: Vinay Singh

Dedicated to

My Grandparents

and

Parents

Acknowledgements

At the outset, I am incredibly grateful to my PhD supervisor Dr D. N. Basu, who reposed faith in my ability to accomplish the work that I was to undertake for PhD. He has been a constant source of encouragement, a never-ending source of energy and has a highly accommodative and helping personality which I am trying to emulate.

It would have been almost impossible to start my research work in Nuclear Astrophysics without the help and support of former Directors of VECC, Dr D. K. Srivastava and Dr Alok Chakrabarti who allowed me to work in a field entirely new for me. I am also indebted to Shri C. Mallik, former Head, APG for encouraging me to pursue for research in any area of my interest.

My wife Maya has been very supportive and encouraging throughout and has been a driving force behind the curtain. I get very emotional at the thought of my children Shiven and Nitika, whom I was not able to give sufficient time given my long engagements with work. My wife and my children thus have a significant share in this work as a lot of their time have been utilized here.

My mother prayers have been a source of hidden strength for me. I can gauge the happiness of my father and my mother when they will get to know about this accomplishment. My brothers, Shri Rakesh and Shri Alok, have always kept my morale up and kept me motivated.

I am indebted to Shri J. S. Prasad, who held my hand and guided me in all times be it of difficulty or otherwise. My sincere thanks to Anuraag who encouraged me to start working for a PhD.

I thank the almighty God, who has provided me with the will to do.

Vinay Singh

Contents

SUMMARY

We present here a robust analytical model based on nuclear reaction theory for non-resonant fusion cross sections near Coulomb barrier. The astrophysical S-factors involving stable and neutron rich isotopes of Carbon, Oxygen, Neon, Magnesium and Silicon for fusion reactions have been calculated in the centre of mass energy range of 2-30 MeV. The model is based on the tunnelling through barrier arising out of nuclear, Coulomb and centrifugal potentials. Our formalism predicts precisely the suppression of S-factor at sub-barrier energies which are of astrophysical interest by using only five parameters for asymmetric systems and just four parameters for symmetric systems and thus providing an accurate and very compact description of S-factor. The cross sections can be convoluted with Maxwell-Boltzmann distribution of energies to obtain thermo- or pycno- nuclear reaction rates relevant to nucleosynthesis at high density environments and stellar burning at high temperatures as well as for ^{34}Ne + ^{34}Ne fusion occurring inside accreting neutron stars in the inner crust region.

The cross sections for deep sub-barrier fusion reaction of light nuclei are calculated within the theoretical framework of selective resonant tunnelling model. In this model, complex square-well form of nuclear potential is assumed to describe absorption inside a nuclear well. The theoretical estimates for these cross sections agree well with the experimentally measured values. The features of the astrophysical S-factor are derived in terms of this model. Present formalism appears to be particularly useful for the low energy resonant reactions between two charged nuclei.

A new reaction rate equation has been developed as a function of T_9 (in units of 10^9 K) by fitting the results for this reaction rate generated from nuclear reaction calculations which turns out to be $N_A < \sigma v >= 389.5 + 218.1 T_9 - 20.21 T_9^2 + 0.853 T_9^3$ cm^{3}s^{-1}mol^{-1}. The results for elemental abundances remained unchanged whether Malaney-Fowler reaction

rate or this new reaction rate or any other reaction rate is used for it. However, this new reaction rate may find its usefulness in other domains of nuclear astrophysics.

The primordial abundance predictions of elements in the BBN is one of the three important pieces of evidence for the big bang model. The other two being the Cosmic Microwave Background Radiation (CMBR) and the Hubble expansion of the Universe. Precise knowledge of the baryon-to-photon ratio of the Universe from observations of the anisotropies of cosmic microwave background radiation has made the Standard BBN a parameter-free theory. Although there is a good consistency between abundances of light elements calculated in primordial nucleosynthesis and those deduced from observations, there still remains an unexplained discrepancy of ^{7}Li which appears to be larger by a factor of ~ 3 when compared with experimental data. The primordial abundances depend on the astrophysical nuclear reaction rates and on three additional parameters, the number of light neutrino flavours, the neutron lifetime and the baryon-to-photon ratio in the universe. The effect of the modification of thirty-five reaction rates on the natural abundances of light elements during the BBN was investigated earlier. In the present work we have incorporated the most recent values of neutron lifetime and the baryon-to-photon ratio and further modified ^{3}He(^{4}He,γ)^{7}Be reaction rate which is used directly for estimating the formation of ^{7}Li as a result of β^{+} decay as well as the reaction rates for t(^{4}He,γ)^{7}Li and d(^{4}He,γ)^{6}Li. We find that these modifications reduce the theoretically calculated abundance of ^{7}Li by $\sim 12\%$.

List of Figures

List of Tables

Chapter 1

INTRODUCTION

1.1 Background, Motivation and Highlights

Ever since their existence, humankind in its endeavour has continuously been trying to decipher the origin of the universe and its constituents in their ultimate goal to know their very own existence. While the Big-Bang theory [1, 2, 3, 4, 5] is one of the most widely accepted theories for our origin [6], a plethora of information still needs to be explored. Our knowledge about elemental abundances is still in a haze, especially about ^{6,7}Li. The observational manifestations of astrophysical processes *viz.* Big-Bang Nucleosynthesis (BBN), Stellar Nucleosynthesis, Supernova explosion and its remnants such as White dwarfs, Neutron stars and Black holes have been a rich source of information for Nuclear Astrophysics.

Nuclear reactions play a vital role in the structure, evolution, nucleosynthesis and various observational manifestations of main-sequence stars, giants and supergiants, pre-supernovae, white dwarfs, and neutron stars. Stellar burning often involves many reactions among different nuclei, from stable to neutron and proton-rich and from light to heavy, rates of which depend on density, temperature and other parameters. These reaction rates can be calculated by using the reaction cross sections $\sigma(E)$. The astrophysical process, however, occurs at very low energies, much below the Coulomb barrier, which exponentially suppresses [7] the cross sections $\sigma(E)$ to the point that it is hardly or not at all measurable. There are cases, in particular involving the weak interaction such as the basic fusion reaction of p+p to deuterium in the solar p-p chain, where no experimental data are available, and one completely relies on theoretical calculations [8]. In general, the laboratory measurements of $\sigma(E)$ are available over a range of energies much higher than those prevalent in stellar interiors and other astrophysical processes. Extrapolation of existing lab measurements is thus often required at energies of astrophysical relevance that are many orders of magnitude smaller. At the same time, $\sigma(E)$ which vary very rapidly with energy leads to concerns about the accuracy of such extrapolations.

Astrophysical S-factor $S(E)$ on the other hand, except for narrow resonances, is comparatively a much slower and a smoothly varying function of energy. So, it is much less prone to extrapolation errors down to low energies of astrophysical interest than cross section $\sigma(E)$. Calculations show that for the reactions between different pairs of interacting nuclei, the theoretical estimates of $S(E)$ [9, 10] can vary by several orders of magnitude. Even for the reaction between the same pair, it may vary by many orders of magnitude in the range of energies of astrophysical relevance. One among the other motivations of the present work is to provide a robust theoretical model of $S(E)$ for non-resonant fusion reactions using a minimum number of parameters and approximations. The astrophysical S-factors involving stable and neutron-rich isotopes of C, O, Ne, Mg and Si for fusion reactions have been calculated using our model [11] in the centre of mass energy range of 2-30 MeV and has been presented in chapter 2.

The model mentioned above, however, cannot incorporate the effect of resonances. This fact motivated to develop a reliable theoretical model which can facilitate extrapolations to energies of astrophysical relevance and is particularly useful for the low energy resonant reactions between two charged nuclei. Calculations have been performed within the theoretical framework of selective resonant tunnelling model where the nuclear resonance not only selects the energy level (frequency) but the damping as well which causes nuclear reactions. Energy dependence of cross sections and astrophysical S-factors for the deep sub-barrier fusion reactions of light nuclei have been calculated using this theoretical model. The astrophysical S-factors for D+D, D+T, D+^{3}He, p+D, p+^{6}Li and p+^{7}Li fusion reactions have been calculated [12] and presented in chapter 3. Improved estimates of these quantities are of prime importance for calculating the elemental abundances in nucleosynthesis.

The extreme conditions of high temperature and pressure occur in the nuclear processes which drive the birth and evolution of stars. The nuclei which make up the majority of matter were first made from nucleons created within a short time after the beginning of the Universe, in the expanding fireball of the Big-Bang, and later forged in the interiors of stars and stellar explosions. The primordial abundance predictions of elements in the BBN is one of the three important pieces of evidence for the big bang model. The other two being the Cosmic Microwave Background Radiation (CMBR) and the Hubble expansion of the Universe. Standard BBN theory predictions depend upon the astrophysical nuclear reaction rates and additionally upon three more parameters, *viz.*, the number of light neutrino flavours, the neutron lifetime and the baryon-to-photon ratio in the Universe. The astrophysical reaction rates are described in detail in chapter 4 while chapter 5 deals with the details of BBN.

Although there is a good consistency between abundances of light elements calculated in primordial nucleosynthesis and those deduced from observations, there still remains an unexplained discrepancy of ^{7}Li which appears to be larger by a factor of ~ 3 when compared experimentally. Calculations have been done by incorporating the most recent values of neutron lifetime and the baryon-to-photon ratio and by further modifying the reaction rates of d(^{4}He,γ)^{6}Li, t(^{4}He,γ)^{7}Li and ^{3}He(^{4}He,γ)^{7}Be. It is found from our studies [13] that the theoretically calculated abundance of ^{7}Li now stands reduced by $\sim$ 12% when compared with the latest available results. It is found from our studies [13] that the theoretically calculated abundance of ^{7}Li now stands reduced by $\sim$ 12% when compared with the latest available results and this has been presented in chapter 6.

In the following the basic definitions, terminology and processes relevant to some aspects of nuclear astrophysics has been described. Though rudimentary, it may be useful in the overall understanding of subject dealt with in this thesis.

1.2 Nuclear reaction cross section and Reaction rate

1.2.1 For Lab events

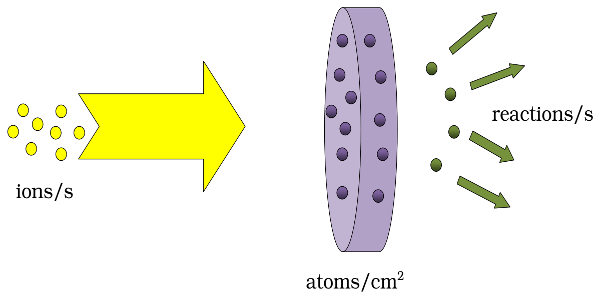

Figure 1.1: Schematic of ions impinging on a target and causing nuclear reaction.

Definition of Nuclear reaction cross section $\sigma(E)$

$$\frac{\text{No. of reactions}}{\text{s}} = \frac{\text{No. of incident particles}}{\text{s}} \times \frac{\text{No. of target nuclei}}{\text{Area}} \times \sigma \tag{1.1}$$

Reaction cross section thus characterizes the probability of a nuclear reaction to occur. Larger the $\sigma(E)$, greater is the probability of reaction. Its dimension is that of area and the unit that we use is barn (b), where 1b $= 10^{-24}$ cm^2 $= 10^{-28}$ m^2.

Reaction rate

For a nuclear reaction between nucleus A and X, the reaction rate r_{AX} is given by

$$r_{AX} = (\sigma N_A)(v N_X) \tag{1.2}$$

where N_X = Number density of nucleus of type X and

N_A = Number density of nucleus of type A

1.2.2 For Astrophysical events

In Astrophysical events, there is a distribution of velocities $\phi(v)$ as opposed to a fixed velocity in experiments. Condition of normalization requires

$$\int_0^\infty \phi(v)\ dv = 1$$

Here the quantity that governs the rate of reaction is $< \sigma v >$. Thus the reaction rate per particle pair for astrophysical events can be obtained by folding with $\phi(v)$ as given below :

$$< \sigma v >= \int_0^\infty (\sigma v)\phi(v)\ dv \tag{1.3}$$

The reaction rate r_{AX} is therefore

$$r_{AX} = \frac{1}{(1+\delta_{AX})} N_X N_A < \sigma v > \tag{1.4}$$

where

$$\delta_{AX} = \begin{cases} 0 & A \neq X \\ 1 & A = X \end{cases}$$

Maxwell – Boltzmann Velocity Distribution

In thermodynamic equilibrium, the Maxwell-Boltzmann distribution of velocities $\phi(v)$ describes the thermal picture of the interacting particles and is given by

$$\phi(v)dv = 4\pi v^2 \left[\frac{\mu}{2\pi kT}\right]^{3/2} \exp\left(-\frac{\mu v^2}{2kT}\right) dv \tag{1.5}$$

where μ is the reduced mass of the interacting nuclei, v is the relative velocity, T is the temperature in Kelvin and k is the Boltzmann constant.

1.3 The Gamow Peak

Substituting Eq.(1.5) in Eq.(1.3), we get

$$< \sigma v >= 4\pi \left[\frac{\mu}{2\pi kT}\right]^{3/2} \int_0^\infty v^3 \sigma(v) \exp\left(-\frac{\mu v^2}{2kT}\right)\; dv \tag{1.6}$$

As the energies involved are non-relativistic, using energy $E = \frac{1}{2}\mu v^2$ in centre-of-mass frame, we get

$$< \sigma v >= \left[\frac{8}{\pi\mu}\right]^{1/2} \left[\frac{1}{kT}\right]^{3/2} \int_0^\infty \sigma(E) \exp\left(-\frac{E}{kT}\right) E\; dE \tag{1.7}$$

Since

$$\sigma(E) = \frac{S(E)\exp(-2\pi\eta)}{E} \tag{1.8}$$

where S(E) is the astrophysical S-factor, Eq.(1.7) reduces to

$$\begin{aligned} < \sigma v >= &\quad \left[\frac{8}{\pi\mu}\right]^{1/2} \left[\frac{1}{kT}\right]^{3/2} \int_0^\infty S(E)\exp(-2\pi\eta) \exp\left(-\frac{E}{kT}\right)\; dE \\ = &\quad \left[\frac{8}{\pi\mu}\right]^{1/2} \left[\frac{1}{kT}\right]^{3/2} \int_0^\infty S(E) \exp\left\{-\left(\frac{E_G}{E}\right)^{1/2}\right\} \exp\left(-\frac{E}{kT}\right)\; dE \end{aligned} \tag{1.9}$$

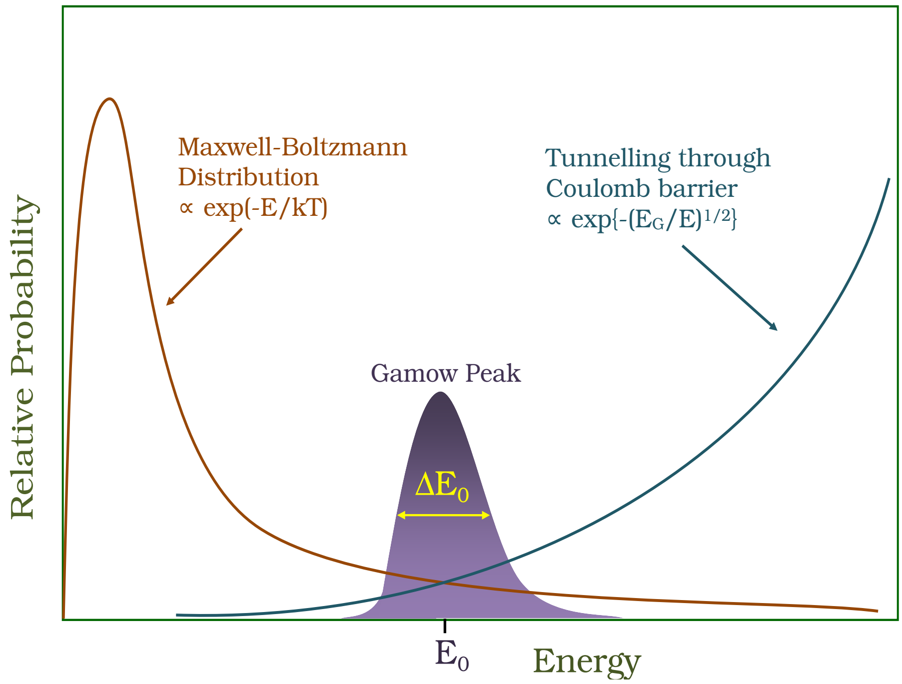

Figure 1.2: Plot showing Maxwell-Boltzmann's distribution, tunnelling probability and Gamow Peak.

Here $\eta = \frac{Z_1 Z_2 e^2}{\hbar v}$ is the Sommerfeld parameter where Z_1 and Z_2 are the atomic numbers of the interacting nuclei, e denotes the elementary charge and $E_G = (2\pi\eta)^2 E$ is the Gamow energy. At particle energies less than the Coulomb barrier the reaction is classically forbidden, but quantum mechanically there is a finite probability for the particle to tunnel through the barrier which is called tunnelling probability. The tunnelling probability is dependent on the term $e^{-2\pi\eta} = e^{-\sqrt{E_G/E}}$ and the particle density is proportional to the term $e^{-E/kT}$. These are the two competing factors: the tunnelling probability increases with increase in energy, whereas the number of particles decreases with increasing energy. It implies that there exists a limited energy range at which most of the reactions occur. This is illustrated in Fig.-1.2; the product of these two exponential terms leads to the 'Gamow peak'. The area under the Gamow peak determines the reaction rate and fusion is most likely to occur in the energy window defined by the Gamow peak [14].

It is worthwhile to mention here that the Gamow peak is not the maximum of the enclosed shaded curve in the figure 1.2, but the entire shaded region. It is named so because it is indeed quite sharply peaked. Therefore, it is a reasonable approximation to assume that the term $S(E)$ is locally constant. The integrand thus peaks at energy E_0, when

$$\begin{aligned}
\frac{d}{dE}\left[\frac{E}{kT}+\left(\frac{E_G}{E}\right)^{1/2}\right] &= \frac{1}{kT}-\frac{1}{2}\left(\frac{E_G}{E_0^3}\right)^{1/2}=0 \\
\Rightarrow \quad E_0 &= \left(\frac{kT\sqrt{E_G}}{2}\right)^{2/3} \\
\Rightarrow \quad E_0 &= \left[\sqrt{2}(\pi\alpha kc)^2\mu(Z_1Z_2T)^2\right]^{1/3} \qquad (1.10)
\end{aligned}$$

the maximum of the Gamow peak E_0 is the most efficient energy for thermonuclear reactions to occur. It is much larger than the typical thermal energy kT but is far below the Gamow energy E_G of the Coulomb barrier.

To calculate the width of the peak, there exists no simple analytical solution. One reasonable and common approach is to approximate the exponential term appearing in the Eq.(1.9) with a Gaussian term centered at E_0. We thus need to solve

$$\exp\left[-\frac{E}{kT}-\left(\frac{E_G}{E}\right)^{1/2}\right] \simeq C\exp\left[-\left(\frac{E-E_0}{\Delta/2}\right)^2\right] \qquad (1.11)$$

where we have used symbol Δ instead σ, as σ has been reserved for cross section in this dissertation. Δ is the full width at $1/e$ of the peak value. Demanding that the two sides be equal at $E = E_0$, we find that

$$C = \exp\left(-\frac{E_0}{kT}-\frac{E_G}{E_0}\right) = \exp\left(-\frac{3E_0}{kT}\right) \qquad (1.12)$$

Now requiring the second derivatives on either side of Eq.(1.11) to be equal results in

$$\Delta = \sqrt{\frac{16}{3}E_0kT} \qquad (1.13)$$

Using Eq.(1.11) and Eq.(1.12) in Eq. (1.9), we get

$$
\begin{aligned}
<\sigma(v)v>= & \left[\frac{8}{\pi\mu}\right]^{1/2}\frac{S(E_0)}{(kT)^{3/2}}\exp\left(-\frac{3E_0}{kT}\right)\int_0^{\infty}\exp\left[-\left(\frac{E-E_0}{\Delta/2}\right)^2\right]dE \\
\simeq & \left[\frac{8}{\pi\mu}\right]^{1/2}\frac{S(E_0)}{(kT)^{3/2}}\exp\left(-\frac{3E_0}{kT}\right)\frac{\Delta\sqrt{\pi}}{2} \qquad (1.14)
\end{aligned}
$$

where the integral has been solved by changing the limit from 0 to $+\infty$ to $-\infty$ to $+\infty$. The error due to this is negligible provided $E_0 > \frac{\Delta}{2}$.

1.4 The Astrophysical S-factor

Nuclear reactions can take place at a rather low temperature in highly dense matter. The energies involved are much below the coulomb barrier leading to very low reaction cross section, but due to high density matter, such reactions do contribute substantially. From the partial wave analysis of formal nuclear reaction theory [15], the cross section for two nuclei undergoing nuclear reaction is given by

$$\sigma(E) = \frac{\pi}{k^2}\sum_{l=0}^{\infty}(2l+1)T_l(E)f_l(E) \qquad (1.15)$$

where $k = \frac{\sqrt{2\mu E}}{\hbar}$, μ being the reduced mass of the interacting nuclei and $T_l(E)$ is the transmission coefficient given by

$$T_l(E) = 1 - |\eta_l|^2 \qquad (1.16)$$

whereas $f_l(E)$ is the fusion probability of the penetrating wave which at low energies of astrophysical interest is close to unity. The quantity $\eta_l = e^{2i\delta_l}$ where δ_l is the phase shift for the l^{th} partial wave. The transmission coefficient $T_l(E)$ can also be expressed as

$$T_l(E) = \exp\left\{-\frac{2}{\hbar}\int_{r_1}^{r_2}\sqrt{2\mu[V_{eff}(r)-E]dr}\right\} \qquad (1.17)$$

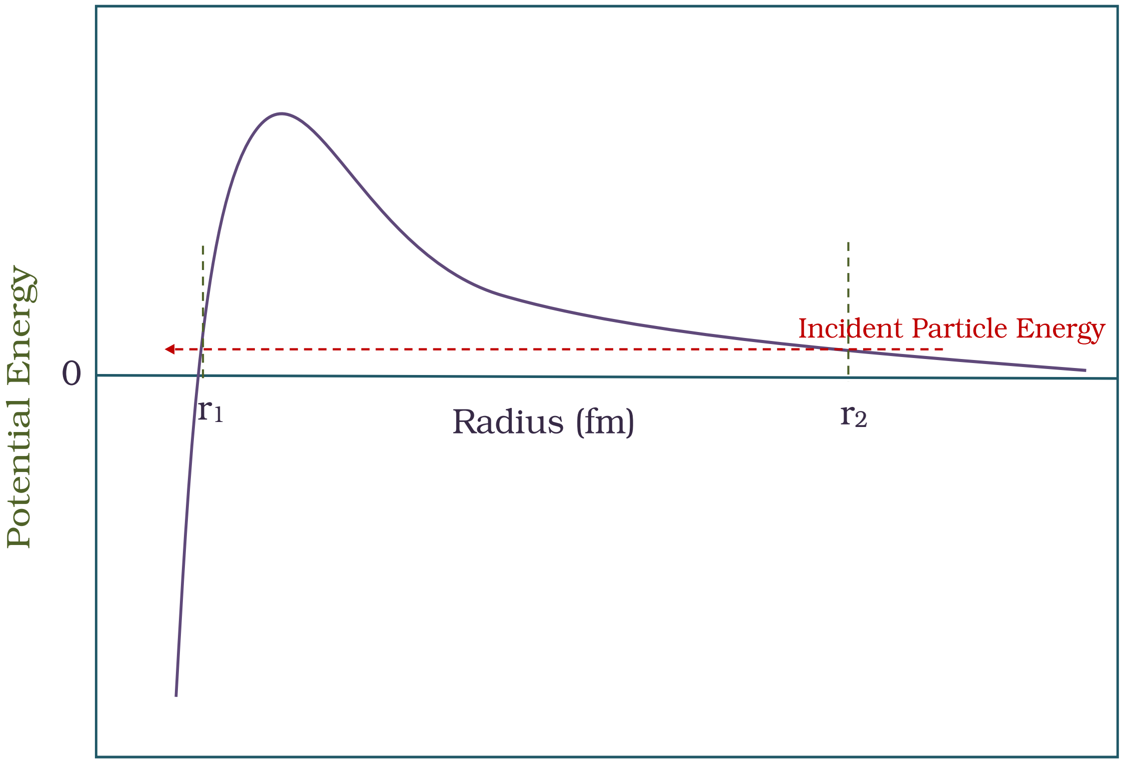

Figure 1.3: Plot showing tunnelling of a particle through a potential barrier and the classical turning points r_1 and r_2.

within WKB approximation, where r_1 and r_2 are classical turning points, E is the energy in the centre of mass frame and $V_{eff}(r)$ is the effective barrier potential given by

$$V_{eff}(r) = V(r) + \frac{l(l+1)\hbar^2}{2\mu r^2} \tag{1.18}$$

The term $V(r)$ in the above equation accounts for the potential energy arising out of nuclear and coulomb force at that value of r. The term $\frac{l(l+1)\hbar^2}{2\mu r^2}$ arises out of centrifugal potential. At low energies, the contribution mainly comes from s-wave (i.e., $l = 0$) making the second term of the above equation to be zero. This approximations can be invoked for solving the integral given by Eq.(1.17). Thus

$$\sigma(E) = \frac{\pi}{k^2} \exp\left\{-\frac{2}{\hbar}\int_{r_1}^{r_2} \sqrt{2\mu[V(r)-E]}\, dr\right\}$$

$$= \frac{\pi}{k^2} \exp\left\{-\frac{2\sqrt{2\mu E}}{\hbar}\int_{r_1}^{r_2}\sqrt{\frac{V(r)}{E}-1}\,dr\right\} \tag{1.19}$$

At the turning point as shown in Fig.-1.3, $r_1 = a$ and $r_2 = b$. Further in the region of our interest, assuming negligible contribution from nuclear force, the contribution to potential $V(r)$ can be taken to come only from coulomb force and therefore, $V(r) = (Z_1 Z_2 e^2)/r$. The value of the integral $\int_{r_1}^{r_2}\sqrt{\frac{V(r)}{E}-1}\,dr$ is $\frac{\pi b}{2}$, whose detailed derivation is presented in the Appendix 1. At the turning point $r_2 = b$, $V(r) = E = (Z_1 Z_2 e^2)/b$. Thus Eq.(1.19) can be rewritten as

$$\begin{aligned} \sigma(E) = & \frac{\pi}{k^2}\exp\left\{-\frac{2\sqrt{2\mu E}}{\hbar}\frac{\pi}{2}\frac{Z_1 Z_2 e^2}{E}\right\} \\ = & \frac{\pi}{k^2}\exp\left\{-2\pi\frac{Z_1 Z_2 e^2}{\hbar v}\right\} \\ = & \frac{\pi}{k^2}\exp\{-2\pi\eta\} \end{aligned} \tag{1.20}$$

where we have used $E = \mu v^2/2$ and $\eta = (Z_1 Z_2 e^2)/\hbar v$ is the Sommerfeld parameter. Now, by using $k^2 = (2\mu E)/\hbar^2$, we can write the Eq.(1.20) as

$$\sigma(E) = \left(\frac{\pi\hbar^2}{2\mu}\right)\frac{1}{E}\exp\{-2\pi\eta\} \tag{1.21}$$

One may write $S_0 = \frac{\pi\hbar^2}{2\mu}$ which is independent of energy. In this derivation nuclear contribution has not been taken explicitly. The obvious generalization of the above behavior of cross section in the low energy domain is

$$\sigma(E) = \frac{S(E)}{E}\exp\{-2\pi\eta\}\,. \tag{1.22}$$

It may be emphasized that astrophysical S-factor $S(E)$ is not the same as S_0 since unlike it, the former takes into account the nuclear contribution and, albeit weak, depends on energy as well. Thus the strong exponential dependence of cross section on center-of-mass energy E caused due to the Coulomb barrier is remedied by the astrophysical S-factor $S(E)$ by factoring out the Coulomb component of the cross section.

1.5 Organization of the Thesis

In chapter 2, the astrophysical S-factors involving stable and neutron-rich isotopes of C, O, Ne, Mg and Si for fusion reactions have been calculated [11] using our model in the centre of mass energy range of 2-30 MeV.

The astrophysical S-factors for D+D, D+T, D+^{3}He, p+D, p+^{6}Li and p+^{7}Li fusion reactions have been calculated [12] and presented in chapter 3.

The astrophysical reaction rates are described in detail in chapter 4 while chapter 5 deals with the details of BBN.

In chapter 6, our studies [13] have found that the theoretically calculated abundance of the ^{7}Li now stands reduced by $\sim 12\%$ when compared with the latest available results.

Finally, concluding remarks have been made in chapter 7.

Chapter 2

NON-RESONANT FUSION REACTIONS OF ASTROPHYSICAL IMPORTANCE

The nuclear reaction cross sections and its convolution with Maxwell-Boltzmann distribution of energies are important for modeling many physical phenomena occurring under extreme conditions [16, 17, 18]. Such environments of very high temperature or density exist in main-sequence stars and compact stars which are in final stages of their evolutionary development. The exothermic nuclear fusion drives nuclear explosions in the surface layers of the accreting white dwarfs (nova events), in the cores of massive accreting white dwarfs (type Ia supernovae) [19, 20] and in the surface layers of accreting neutron stars (type I X-ray bursts and superbursts [21, 22, 23, 24]). The type-I X-ray bursts and the nova events are generally produced by stellar burning of hydrogen in the thermonuclear regime, without significant effect of plasma screening on the Coulomb tunnelling of interacting nuclei. The superbursts and type Ia supernovae are driven by the burning of C, O, Ne, Si and heavier elements [21, 22, 23, 24] at high densities, where the plasma screening effect may be significant. In the inner crust of accreting neutron stars (in binaries with low-mass companions [24, 25, 26]) the pycnonuclear burning of neutron rich nuclei such as ^{34}Ne + ^{34}Ne is most likely the source of their internal heat. All these astrophysical processes require precise knowledge of nuclear reaction rates.

The thermonuclear reaction rates can be obtained by convoluting fusion cross sections with Maxwell-Boltzmann distribution of energies. These cross sections can vary by several orders of magnitude across the required energy range. The sharp energy dependence of these cross sections can be accounted by an exponential factor while the astrophysical S-factor is a smooth slowly varying function of energy facilitating its extrapolation down to astrophysical energies. The low energy fusion cross sections σ, some of which are not sufficiently well known, can be obtained from laboratory experiments. The theoretical estimations of thermonuclear reaction rates is dependent on the use of various approximations. Several factors influence the experimentally measured cross section values. We need to take into account the Maxwellian-averaged thermonuclear reaction rates in the network calculations used in Big-Bang and stellar nucleosynthesis.

At energies much below the Coulomb barrier, the radius of the nucleus is too small compared to the classical turning point. In this situation $\exp(-2\pi\eta)$ approximates the tunnelling probability through the barrier quite well, where $\eta = \frac{Z_1 Z_2 e^2}{\hbar v}$ is the Sommerfeld parameter with Z_1 and Z_2 being the atomic numbers of the interacting nuclei and e being the elementary charge. As a consequence, the charge induced cross section can be factorized as

$$\sigma(E) = \frac{S(E)\exp(-2\pi\eta)}{E} \tag{2.1}$$

where E is the energy measured in the centre-of-mass frame, $S(E)$ is the astrophysical S-factor which is a smoothly varying function of energy (as long as the narrow resonances are excluded) and hence facilitating extrapolation of experimentally measured cross sections down to the energies of astrophysical interest. For narrow resonance cases, in general a Breit-Wigner expression approximates the resonant cross section, whereas at low energies the cross sections of neutron induced reactions is given by $\sigma(E) = \frac{R(E)}{v}$ [15] with $R(E)$ being a slowly varying function of energy [27] is similar to S-factor.

Depending on the temperature and the density, along with other parameters, stellar burning may involve reactions of different kind from light to heavy nuclei, and from stable to unstable proton or neutron rich. The rates of these reactions can be calculated from the reaction cross sections σ by folding it with a Maxwell-Boltzmann energy distribution corresponding to the plasma temperature T. The Maxwellian-averaged thermonuclear reaction rate thus obtained can now be given by the following integral [8, 28]:

$$< \sigma v >= \Big[\frac{8}{\pi\mu(k_B T)^3}\Big]^{1/2} \int \sigma(E) E \exp(-E/k_B T) dE, \tag{2.2}$$

for per particle pair at temperature T with μ being the reduced mass of the reacting nuclei and v being the relative velocity. Therefore, the reaction rate between two nuclei can be written as $r_{12} = \frac{n_1 n_2}{1+\delta_{12}} < \sigma v >$ where n_1 and n_2 are the number densities of nuclei of types 1 and 2. The Kronecker delta δ_{12} prevents double counting in the case of identical particles.

The nuclear fusion reactions at very low energies play the most important role in the nucleosynthesis of light elements in big bang nucleosynthesis as well as nuclear burning inside the stellar core. In the present work, we have calculated $S(E)$ for a number of fusion reactions of astrophysical importance. The theoretical formulation is based on barrier penetration model. The barrier arising out of nuclear and Coulomb potentials is assumed to be of parabolic shape and the centrifugal barrier is added to it. The energy dependence of the cross sections and astrophysical S-factors for the fusion reactions

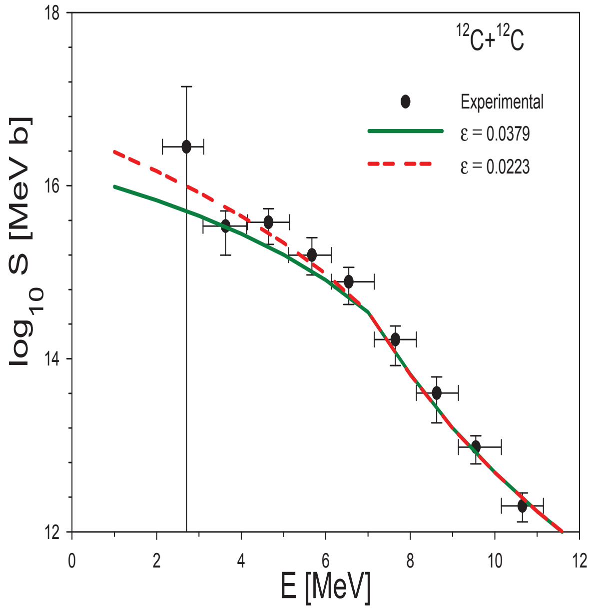

Figure 2.1: Plots of S-factors for C+C fusion reaction. The filled dots with error bars represent the experimental data points [29, 30, 31, 32, 33, 34, 35, 36, 37, 38, 39, 40] while the solid and the dashed lines are our present calculations corresponding to two ε values.

involving stable and several neutron rich isotopes of C, O, Ne, Mg and Si covering a wide range of energy from 2 MeV to 30 MeV, below and above the Coulomb barrier, have been calculated using this model and compared with the experimentally measured data [29, 30, 31, 32, 33, 34, 35, 36, 37, 38, 39, 40].

2.1 Theoretical foundation

The knowledge of astrophysical S-factor $S(E)$ for numerous nuclear reactions is the prime requirement for explaining various astrophysical phenomena. The experimental measurements of cross sections $\sigma(E)$ at energies involved are quite often not available due to the fact that the Coulomb barrier suppresses exponentially the cross sections at low energies. The nuclear physics uncertainties of the calculated $S(E)$ can be significant since the theoretical calculations are model dependent. The calculations show that for the reactions

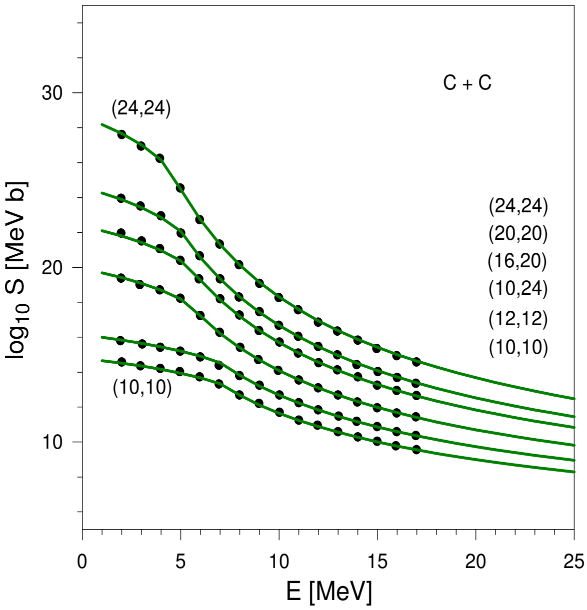

Figure 2.2: Plots of S-factors for six C+C fusion reactions. The filled dots are the São Paulo (SP) [10] calculations while the solid lines are our present calculations (see Table-2.1).

between different pairs of interacting nuclei, the theoretical estimates of $S(E)$ [9, 10] can vary by several orders of magnitude. Even for the reaction between the same pair it may vary by many orders of magnitude in the range of energies of astrophysical relevance. The primary motivation of this work is to provide a robust theoretical model of $S(E)$ for non-resonant fusion reactions using minimum number of parameters and approximations.

The present theoretical model is based on the theory of inelastic scattering [41]. The reaction cross section has been derived accordingly. The transmission coefficient T_l for $l = 0$ is calculated assuming quantum mechanical barrier penetration. The potential barrier arising due to nuclear and Coulomb interactions has been assumed to be of a parabolic form. The height and the slope of the barrier are matched at a matching radius R_m greater than the radius R_c at which the barrier peaks by an amount characterized by ε. The transmission coefficients for $l > 0$ are calculated from physical consideration which accounts for the effect of the centrifugal barrier as well.

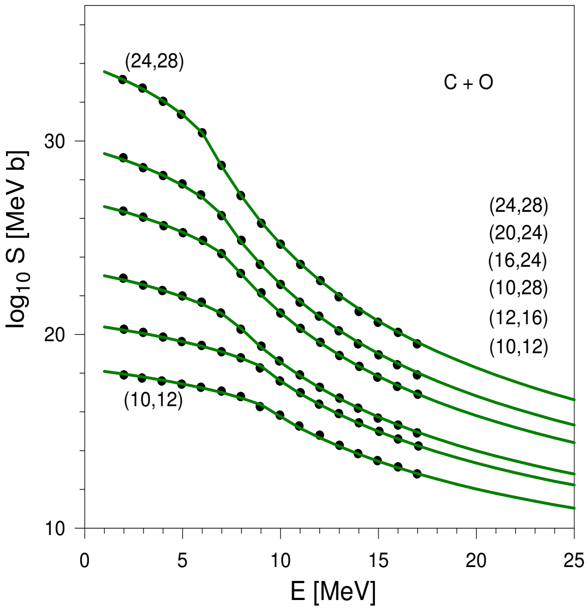

Figure 2.3: Plots of S-factors for six C+O fusion reactions. The filled dots are the São Paulo (SP) [10] calculations while the solid lines are our present calculations (see Table-2.1).

2.1.1 Ion-ion Nuclear and Coulomb potentials

We select an inverse parabolic form for the barrier potential arising due to nuclear and Coulomb interactions. The nuclear force being short range, it is assumed to be an inverse parabolic potential at radial separation $r < R_m$ and pure Coulomb potential beyond:

$$V(r) = \begin{cases} \frac{\lambda}{r} & \forall \;\; r \geq R_m \\ E_c\Big[1 - \zeta\frac{(r-R_c)^2}{R_c^2}\Big] & \forall \;\; r < R_m \end{cases} \tag{2.3}$$

where $\lambda = Z_1 Z_2 e^2$, E_c is the maximum height of the barrier at $r = R_c$ and ζ defines the parabolic shape of the barrier. We demand that the logarithmic derivative of the potential to be continuous to have a very smooth change of the force. This implies that $V(r)$ and $\frac{dV(r)}{dr}$ be continuous at $r = R_m$ which yield

$$
\begin{aligned}
E_c &= V(R_c) = \frac{\lambda(2+3\varepsilon)}{2R_c(1+\varepsilon)^2}, \qquad \zeta = [\varepsilon(2+3\varepsilon)]^{-1}, \\
E_m &= V(R_m) = E_c\frac{2(1+\varepsilon)}{2+3\varepsilon} \;\; \text{where} \;\; \varepsilon = \frac{(R_m - R_c)}{R_c}.
\end{aligned} \tag{2.4}
$$

Thus the model is very natural and realistic [42] as well, which allows one to obtain analytic expressions for the barrier penetrability.

2.1.2 Quantum tunnelling and fusion cross section

The basic picture of the analytical model is that the fusion cross section can be given by the formal nuclear reaction theory [15]

$$
\sigma(E) = \frac{\pi}{k^2}\sum_{l=0}^{\infty} (2l+1)T_l(E)f_l(E) \tag{2.5}
$$

where $k = \frac{\sqrt{2\mu E}}{\hbar}$, μ being the reduced mass of the interacting nuclei and $T_l(E)$ is the transmission coefficient given by

$$
T_l(E) = 1 - |\eta_l|^2 \tag{2.6}
$$

whereas $f_l(E)$ is the fusion probability of the penetrating wave which at low energies of astrophysical interest is close to unity. The quantity $\eta_l = e^{2i\delta_l}$ where δ_l is the phase shift for the l^{th} partial wave. The phase shift δ_l has to have a finite imaginary part in order to find a transmission coefficient T_l different from zero. In the energy domain involved, the transmission coefficient $T_l(E)$ decreases with l and the largest contribution comes from the $T_0(E)$ term suggesting one to introduce a quantity $N(E)$ such that

$$
N(E) = 1 + \sum_{l=1}^{\infty} (2l+1)\frac{T_l(E)}{T_0(E)} \tag{2.7}
$$

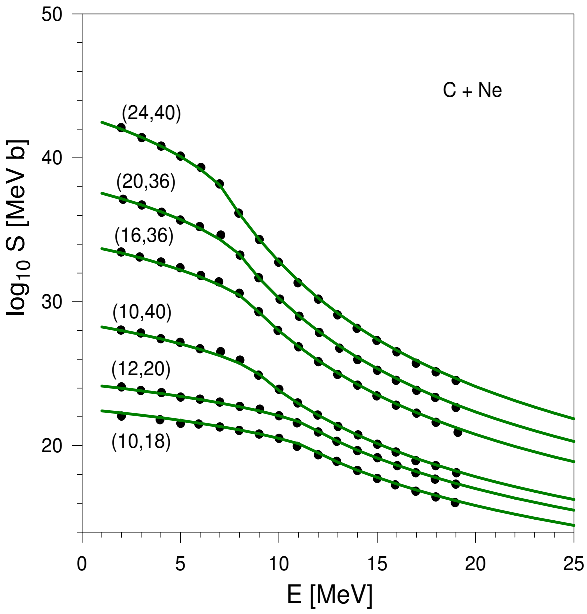

Figure 2.4: Plots of S-factors for six C+Ne fusion reactions. The filled dots are the São Paulo (SP) [10] calculations while the solid lines are our present calculations (see Table-2.1).

whose magnitude is expected to be larger than unity due to the contributions from higher partial waves.

Substituting Eq.(2.7) in Eq.(2.5) one finds that

$$\sigma(E) = \frac{S_0}{E} N(E) T_0(E) \tag{2.8}$$

where $S_0 = \frac{\pi\hbar^2}{2\mu}$ and the s-wave transmission coefficient

$$T_0(E) = \exp\Big\{ -\frac{2}{\hbar}\int_{r_1}^{r_2} \sqrt{2\mu[V(r)-E]}dr\Big\} \tag{2.9}$$

where r_1 and r_2 are classical turning points. Prompted by Eq.(2.1), expressing $T_0(E)$ as $\exp(\Theta - 2\pi\eta)$, analytical expressions can be derived for Θ for the barrier potential given by Eq.(2.3) which for $0 \le E < E_m$ given by

$$\Theta(E) \;\; = \;\; 4\sqrt{\frac{E_r}{E}}\Big[\sin^{-1}\sqrt{y_r} + \sqrt{y_r(1-y_r)}\Big] \tag{2.10}$$

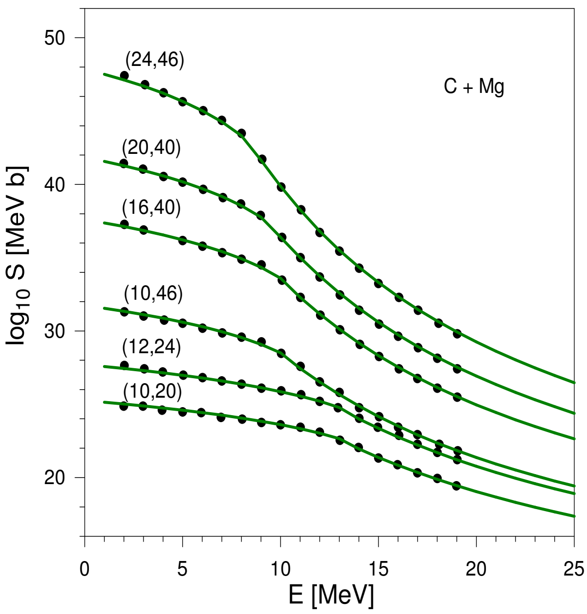

Figure 2.5: Plots of S-factors for six C+Mg fusion reactions. The filled dots are the São Paulo (SP) [10] calculations while the solid lines are our present calculations (see Table-2.1).

$$- \quad \xi\sqrt{\frac{E_r}{E_c}}\frac{(E_c - E)}{E_c}\Big[\frac{\pi}{2} + \sin^{-1} y_l + y_l\sqrt{1 - y_l^2}\Big]$$

and for $E_m \leq E \leq E_c$ given by

$$\Theta(E) = \pi\Big[2\sqrt{\frac{E_r}{E}} - \xi\frac{(E_c - E)}{E_c}\sqrt{\frac{E_r}{E_c}}\Big] \tag{2.11}$$

where $y_r = \frac{R_m E}{\lambda}$, $y_l = \varepsilon\sqrt{\frac{\zeta E_c}{E_c - E}}$, $E_r = \frac{\lambda^2\mu}{2\hbar^2}$ and $\xi = \frac{(2+3\varepsilon)^{3/2}\sqrt{\varepsilon}}{(1+\varepsilon)^2}$.

The expressions provided above are for sub-barrier energies where the S-factor is influenced by several low l values at $E \leq E_c$ in which $l = 0$ contributing the most. The correcting factor $N(E)$ is expected to be a slowly varying function of energy. It is likely that the transmission coefficients $T_l(E)$ at these l values are similar functions of energy as T_0 but of strengths reducing progressively with increasing l implying s-wave like energy dependence. A crude estimate for $N(E)$ at $E \leq E_c$ goes as $\sim 1 + \sqrt{\frac{E_c}{E_0}}$ [43]. To simplify the model it is assumed that $N(E)$ can be approximated by an overall normalization factor

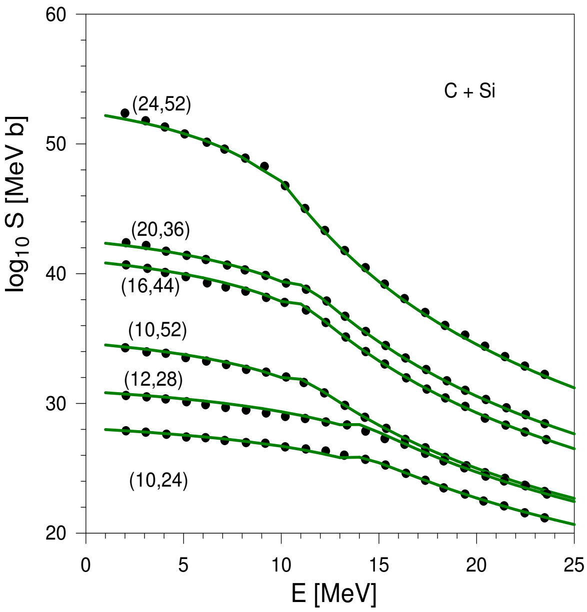

Figure 2.6: Plots of S-factors for six C+Si fusion reactions. The filled dots are the São Paulo (SP) [10] calculations while the solid lines are our present calculations (see Table-2.1).

$$N(E) \approx N_0 = 1 + n_0\sqrt{\frac{E_c}{E_0}} \tag{2.12}$$

where $E_0 = \frac{\hbar^2}{2\mu R_c^2}$ is the characteristic quantum of centrifugal energy and n_0 can be treated as a parameter characterizing the significance of higher partial waves.

For above barrier energies $E > E_c$ the effective barrier is transparent for low l waves resulting $T_l = 1$. The summation over partial waves in the expression of cross section provided by Eq.(2.5) goes from $l = 0$ to maximum $l = l_m$ at which the effective barrier $V(r) + \frac{\hbar^2 l(l+1)}{2\mu r^2}$ becomes classically forbidden. In this case a simplified derivation [43] yields

$$\Theta(E) = 2\pi\eta + \frac{1}{2}\ln\Big[1 + \frac{y^2(E)}{N_0^2}\Big] \tag{2.13}$$

where $y(E) = \frac{(E-E_c)}{E_0}\Big[1 - \frac{(E-E_c)}{\zeta E_c}\Big]$.

Recalling the definition from Eq.(2.1), the S-factor can be given by

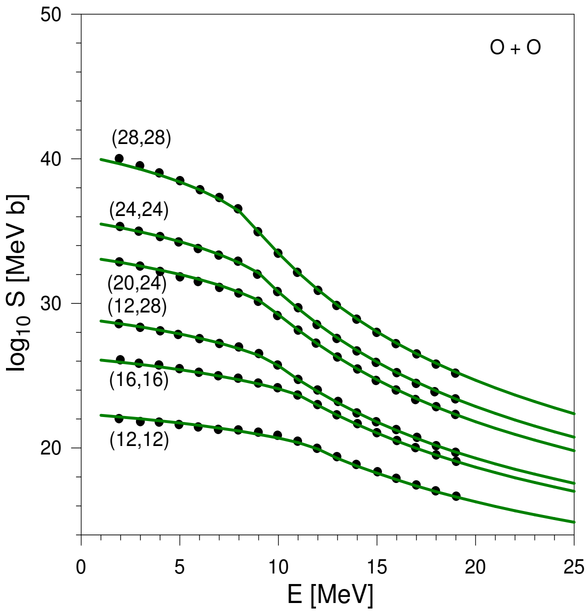

Figure 2.7: Plots of S-factors for six O+O fusion reactions. The filled dots are the São Paulo (SP) [10] calculations while the solid lines are our present calculations (see Table-2.1).

$$S(E) = N_0 S_0 \exp \Theta(E) \tag{2.14}$$

where the expressions of $\Theta(E)$ for different energy domains have been provided by Eq.(2.10), Eq.(2.11) and Eq.(2.13).

2.2 Calculation of astrophysical S-factor

The calculation of astrophysical S-factor using present formalism involves five parameters. The barrier potential is defined by R_c and ζ (or equivalently ε) since barrier height E_c can be expressed in terms of R_c and ε. The radius at which the barrier peaks can be given in terms of the mass numbers A_1 and A_2 of the interacting nuclei by $R_c = r_0(A_1^{1/3} + A_2^{1/3}) + |A_1 - 2Z_1|\Delta_1 + |A_2 - 2Z_2|\Delta_2$ which involves three parameters. The isotopic dependence of R_c is simulated by entities $\Delta_{1,2}$ and r_0 is the radius parameter. The fifth parameter

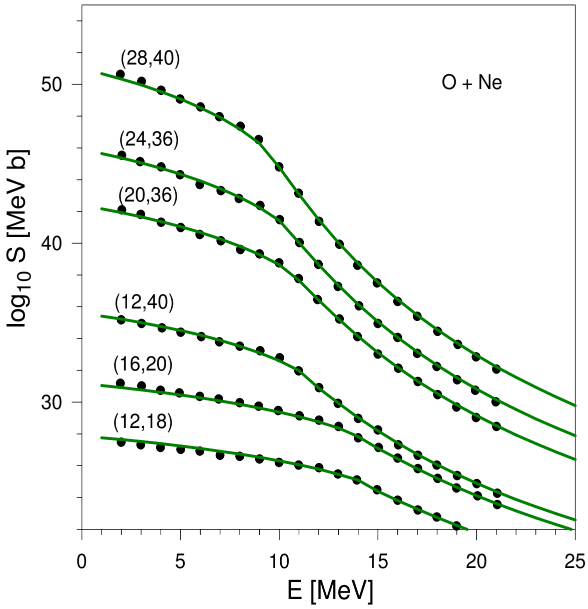

Figure 2.8: Plots of S-factors for six O+Ne fusion reactions. The filled dots are the São Paulo (SP) [10] calculations while the solid lines are our present calculations (see Table-2.1).

n_0 characterizes the effect of partial waves $l > 0$. The present formalism causes two fold simplifications: it reduces two parameters and relies on exact theoretical expressions for barrier penetration rather than the approximated ones [43, 44]. The five parameters for various fusing systems have been obtained by fitting the astrophysical S-factors from experimental measurements and theoretical results of a nine-parameter phenomenological analytic expression [10] which were also compared previously [9, 45, 46] with experimental data wherever available. The errors in the fitted parameters are calculated from the correlation matrix in the final stage of the fitting procedure when changes in the fitted parameters by amounts equal to the corresponding uncertainties in the fitted parameters cause changes in the corresponding quantity by less than the stipulated value. Thus large uncertainty in a fitted parameter implies that the hyper-surface is rather flat with respect to that parameter.

Table 2.1: Values of parameters for S(E) for various isotopes of reactions

Reactions	r_0 (fm)	ε	n_0	Δ_1 (fm)	Δ_2 (fm)
C+C	1.5223 ±0.0084	0.0379 ±0.0015	1.7982 ±0.1027	0.1006 ±0.0013	0.1006 ±0.0013
C+O	1.5346 ±0.0054	0.0360 ±0.0010	1.9156 ±0.0913	0.0967 ±0.0012	0.0549 ±0.0008
C+Ne	1.4857 ±0.0082	0.0326 ±0.0014	2.3993 ±0.1775	0.1150 ±0.0017	0.0548 ±0.0007
C+Mg	1.5162 ±0.0053	0.0401 ±0.0008	1.7216 ±0.1192	0.0915 ±0.0009	0.0524 ±0.0004
C+Si	1.6732 ±0.0038	0.0531 ±0.0007	0.0975 ±0.0134	0.0602 ±0.0012	0.0481 ±0.0005
O+O	1.5766 ±0.0057	0.0410 ±0.0008	1.5939 ±0.0985	0.0527 ±0.0009	0.0527 ±0.0009
O+Ne	1.5628 ±0.0049	0.0423 ±0.0008	1.3828 ±0.1007	0.0606 ±0.0009	0.0555 ±0.0004
O+Mg	1.5712 ±0.0054	0.0450 ±0.0007	0.7472 ±0.0639	0.0481 ±0.0010	0.0491 ±0.0004
Ne+Ne	1.5036 ±0.0055	0.0387 ±0.0008	2.1797 ±0.2504	0.0585 ±0.0004	0.0585 ±0.0004
Ne+Mg	1.5237 ±0.0072	0.0443 ±0.0010	1.7510 ±0.1981	0.0720 ±0.0005	0.0399 ±0.0004
Mg+Mg	1.4791 ±0.0066	0.0387 ±0.0007	1.2801 ±0.1959	0.0473 ±0.0004	0.0473 ±0.0004

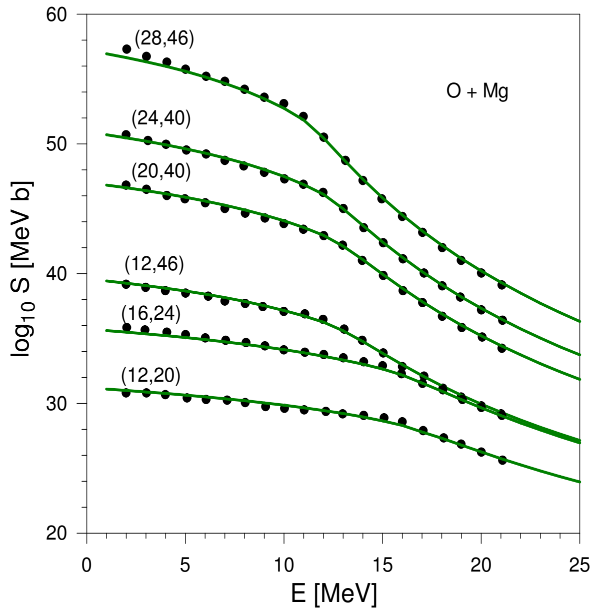

Figure 2.9: Plots of S-factors for six O+Mg fusion reactions. The filled dots are the São Paulo (SP) [10] calculations while the solid lines are our present calculations (see Table-2.1).

2.3 Results and discussion

The astrophysical S-factors involving stable and neutron rich isotopes of C, O, Ne, Mg and Si for fusion reactions have been calculated in the centre of mass energy range of 2-30 MeV. The experimental measurements of ^{12}C+^{12}C reaction cross sections have also been performed by various groups. The fusion cross section for ^{12}C+^{12}C system is the sum of the cross sections for proton, α and neutron channels where contributions from the first two channels are substantial. These cross sections contain both resonances and the non-resonant part. The present theoretical calculations can be compared with the non-resonant contribution only. Therefore, for comparison with the present theoretical model the experimental data for $S(E)$ have been chosen selectively from Refs.[29, 30, 31, 32, 33, 34, 35, 36, 37, 38, 39, 40] which cover the range of energies from $\approx$ 2 MeV to 20 MeV. These data are not fully consistent and somewhat non uniform, particularly in

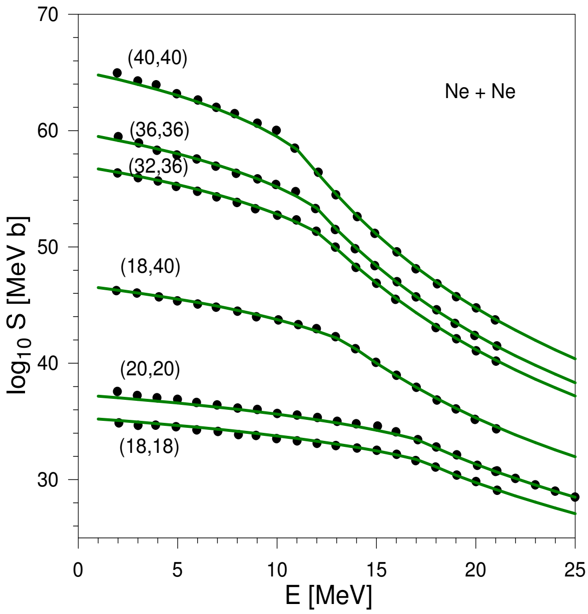

Figure 2.10: Plots of S-factors for six Ne+Ne fusion reactions. The filled dots are the São Paulo (SP) [10] calculations while the solid lines are our present calculations (see Table-2.1).

the lower energy range, where experimental $S(E)$ measurements are most difficult and experimental uncertainties are high. The experimental values of $S(E)$ are rather uncertain at lower energies, moderately uncertain in the energy range of 3 - 4 MeV and seem to be reasonably accurate at energies ≥ 4 MeV. The data analysis becomes complicated due to the presence of low-energy resonances [38, 40].

In order to compare with the present theoretical calculations, which do not take into account the resonances, and to smooth out the effect of experimental uncertainties, the experimental data have been binned with 1 MeV width [44]. The binned data are shown by crosses (filled dots with error bars) in the Fig.-2.1. In Fig.-2.1 the S-factors for $^{12}C+^{12}C$ fusion reaction have been plotted as a function of centre of mass energy of the colliding nuclei. The filled dots with error bars represent the experimental data points [29, 30, 31, 32, 33, 34, 35, 36, 37, 38, 39, 40]. The solid line represents our present calculations fitted to the São Paulo (SP) [10] calculations. The dashed line has been fitted to the

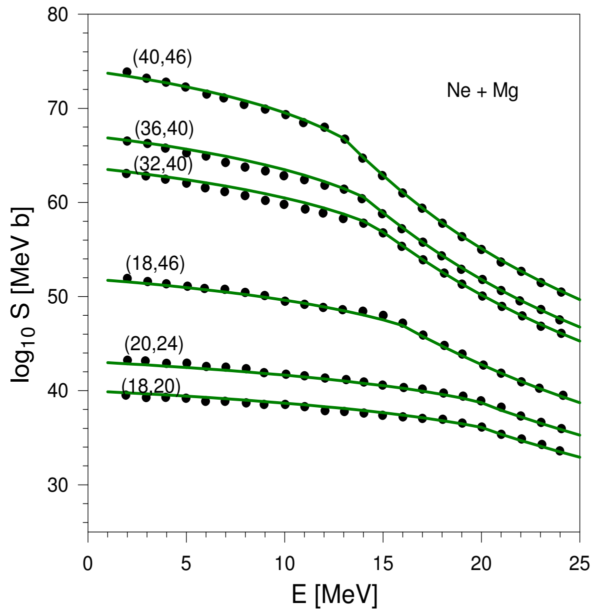

Figure 2.11: Plots of S-factors for six Ne+Mg fusion reactions. The filled dots are the São Paulo (SP) [10] calculations while the solid lines are our present calculations (see Table-2.1).

experimental data by just varying the value of ε while keeping the other four parameters identical as provided in Table-2.1 for C+C system. This exercise has been done to show that the parameters extracted by fitting the São Paulo (SP) [10] results are good enough for predictions of astrophysical S-factors. In Figs.-2.2-2.12, plots of S-factors for various isotopes of C, O, Ne, Mg and Si for fusion reactions have been plotted as a function of centre of mass energy. The filled dots are the São Paulo (SP) [10] calculations while the solid lines are our present calculations. The parameter sets for these reactions are listed in Table-2.1.

We find that the standard errors in the fitted parameters are minimum for r_0 and ε and maximum for n_0. This implies that the results of the calculations are most sensitive to r_0 and ε and least sensitive to n_0. The sensitivity of Δ_1 and Δ_2 on $S(E)$ indicates a possible path of finding isotopic dependence of nuclear radius. The results of the present calculations show that the same set of the five parameters as stated can provide good es-

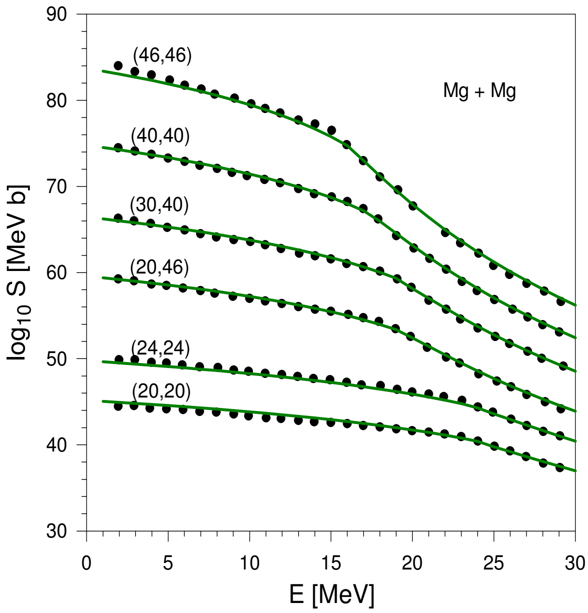

Figure 2.12: Plots of S-factors for six Mg+Mg fusion reactions. The filled dots are the São Paulo (SP) [10] calculations while the solid lines are our present calculations (see Table-2.1).

timates of $S(E)$ for the entire range of isotopes for a particular combination of interacting nuclei. In case of same nuclei such as C+C or Mg+Mg, the number of parameters further reduces from five to four since in these cases $\Delta_1 = \Delta_2$. Moreover, the present formalism not only removes two parameters of Ref.[43] but also relies on exact theoretical expressions for barrier penetration rather than the approximated ones used in Refs.[43, 44].

2.4 Summary and conclusion

In this work, we present analytical formulation based on barrier penetration model for the astrophysical S-factor $S(E)$. The potential barrier due to nuclear and Coulomb interactions has been assumed to be of parabolic nature. The effect of the centrifugal barrier for $l > 0$ which in turn means the contributions from higher l values have been simulated phenomenologically. Except for this, the entire formulation is exact and does not invoke any other approximation. However, the issue of strong variation with the energy [47] due to possible resonances, which could not be encompassed in earlier works [10, 43, 44] as well, still remains but the present endeavor causes two fold simplifications. It reduces two parameters and relies on exact theoretical expressions for barrier penetration rather than the approximated ones [43, 44]. The energy dependence of the astrophysical S-factors for the fusion reactions involving stable and several neutron rich isotopes of C, O, Ne, Mg and Si covering a wide range of energy from 2 MeV to 30 MeV, below and above the Coulomb barrier, have been calculated. The mentioned reactions are merely a few illustrative examples, but the elegance of the theoretical model in describing the experimental data suggests that it may be used successfully for large number of other nuclei encompassing the entire spectra of isotopes.

Chapter 3

RESONANT FUSION REACTIONS IN ASTROPHYSICS

The cross sections for deep sub-barrier fusion reaction of light nuclei are calculated within the theoretical framework of selective resonant tunnelling model. In this model, assumption of a complex square well potential for nuclear interaction is invoked to explain the absorption inside a nuclear potential well. The theoretical estimates for these cross sections agree well with the experimentally measured values. The features of the astrophysical S-factor are derived in terms of this model. Present formalism appears to be particularly useful for the low energy resonant reactions between two charged nuclei.

Nuclear fusion reactions at very low energies plays important role in nucleosynthesis of light elements in big bang nucleosynthesis as well as inside the stellar core. Fusion cross section is also one of the most important physical quantity required for both design and research in fusion engineering. Nuclear fusion reactions in the energy range of $\sim$1eV to few keV can be explained successfully by the phenomenon of quantum mechanical tunnelling through Coulomb barrier of interacting nuclei. The measurements of these cross sections of astrophysical importance are rarely possible since the energies involved in these processes are extremely low causing its exponential suppression due to coulomb barrier. The astrophysical S-factor which is related to cross section [Eq.(2.1)] is, however, a slowly varying function and is much less prone to extrapolation errors down to low energies of astrophysical interest than cross section which has sharp energy dependence owing to the exponential factor. Primary motivation of this work is to provide a reliable theoretical model which can facilitate such extrapolations. Energy dependence of cross sections and astrophysical S-factors for the deep sub-barrier fusion reactions of light nuclei have been calculated using the theoretical model. In the present work, the astrophysical S-factors for D+D, D+T, D+^{3}He, p+D, p+^{6}Li and p+^{7}Li fusion reactions have been calculated whose improved estimates are of prime importance for calculating the elemental abundances in nucleosynthesis.

3.1 Theoretical framework

In the present work, a simple square-well potential model with an imaginary part has been used to describe the nuclear fusion reaction of light nuclei where the nuclear potential's real part is primarily derived from the resonance energy whereas its imaginary part is determined by Gamow factor at the resonance energy. This complex square-well nuclear potential describes the absorption inside the nuclear well. In case of light nuclei fusion, treating the resonant tunnelling through the Coulomb barrier as a two-step process, that is, first tunnelling and then decay, fails to provide an adequate description. Such a oversimplified one-dimensional model [48], based on the assumption of decay being independent of tunnelling, does not depict a true picture of the physical process. In reality, the wave function of the system of two colliding nuclei reflects back and forth inside the nuclear potential well after it penetrates the barrier. These reflections inside the nuclear well are completely neglected in the one dimensional model where the wave suffers no reflection while penetrating the barrier. In the case of α-decay as well, the outgoing α-particle will encounters no reflection after penetrating the barrier in a three dimensional model [49]. While the decay of the penetrating nuclei terminates the bouncing motion inside the nuclear well, if nuclear reaction happens quickly enough, the wave function will have no time to execute this bouncing motion. In other words, the short lifetime of the penetrating wave may forbid resonant tunnelling. This is because of the fact that there will be not enough bouncing motion for the growth of the wave function by means of constructive interference inside the nuclear well. The tunnelling and decay can no longer be independent in light nuclear fusion process and need to be combined as a selective process.

The lifetime effect on the resonant tunnelling can be best achieved by introducing an imaginary part into the nuclear interaction potential. The complex nuclear potential has been shown to describe successfully the resonant tunnelling effects in deep sub-barrier fusion using a three dimensional model for wide range of energies [50, 51, 52]. It is actually the overcoming of Gamow tunnelling insufficiencies by maximizing a damp-matching resonant tunnelling. This theory is called the 'selective resonant tunnelling' and was originally developed by Xing Zhong Li et al. [52]. When a light nucleus is injected into another, the reduced radial wave function $\psi(r)$ describing the relative motion can be related to the full wave function $\Phi(r,t) = \frac{1}{\sqrt{4\pi}r}\psi(r)\exp(-i\frac{E}{\hbar}t)$. Here, $\Phi(r,t)$ represents the solution of the general Schrödinger equation for the system. The reaction cross section in terms of the phase shift δ_0 due to the nuclear potential (in low energy limit only s-wave contributes) is given by $\sigma = \frac{\pi}{k^2}[1-|\eta_0|^2]$ where $\eta_0 = e^{2i\delta_0}$ and $k = \sqrt{\frac{2\mu E}{\hbar^2}}$ is the relative motion wave number between the reacting nuclei. In the three dimensional calculation, nuclear potential being complex, the corresponding phase shift δ_0 is complex and is given by [52]

$$\cot(\delta_0) = W_r + iW_i \tag{3.1}$$

where instead of conventional phase shift δ_0, a new pair of parameters, W_r and W_i, the real and the imaginary parts of the cotangent of phase shift have been introduced. Consequently, the reaction cross section for the s-wave given by $\sigma = \frac{\pi}{k^2}\left(1 - |e^{2i\delta_0}|^2\right)$ can be rewritten as

$$\begin{aligned} \sigma &= \frac{\pi}{k^2}\left\{-\frac{4W_i}{(1-W_i)^2 + W_r^2}\right\} \\ &= \left(\frac{\pi}{k^2}\right)\left(\frac{1}{\chi^2}\right)\left\{-\frac{4\omega_i}{\omega_r^2 + (\omega_i - \frac{1}{\chi^2})^2}\right\} \end{aligned} \tag{3.2}$$

where $\chi^2 = \left\{\frac{\exp\left(\frac{2\pi}{ka_c}\right)-1}{2\pi}\right\}$ and $1/\chi^2$ is the Gamow penetration factor, $\omega = \omega_r + i\omega_i = W/\chi^2 = (W_r + iW_i)/\chi^2$ and $a_c = \hbar^2/\mu Z_1 Z_2 e^2$ is the length of Coulomb unit. The above expression is for inclusive cross section in which all the exit channels are summed over. Since only the fusion cross section is being calculated, explicit treatment to incorporate exit channels has not been taken into account. It is evident that the cross section reaches its maximum when $W_r = 0$ and $W_i = -1$ and $W_r = 0$ corresponds to the condition for resonance. Thus the condition for resonance is $\mathrm{Re}(\delta_0) = (2n+1)\pi/2$ where n is an integer. The dimensionless quantity $S_r(E)$ given by

$$S_r(E) = \left\{-\frac{4\omega_i}{\omega_r^2 + (\omega_i - \frac{1}{\chi^2})^2}\right\} \tag{3.3}$$

provides an alternative expression for a dimensionless astrophysical S-function which is related to the astrophysical S-factor $S(E)$ by $S(E)=\frac{\pi\hbar^2 \exp(2\pi\eta)}{2\mu\chi^2} S_r(E)$. The two parameters V_r and V_i which are respectively the real and imaginary parts of nuclear potential, determine the wave function inside the nuclear well. Outside the potential well of the nucleus, Coulomb wave function is determined by two parameters: $(\delta_0)_r$ and $(\delta_0)_i$ which are respectively the real and the imaginary parts of the complex phase shift. The derivation of Eq.(3.4) does not invoke 'compound nucleus model', rather it contains not only the conventional Gamow factor at front but also has an energy dependence of the S-factor (or the astrophysical S-function). It is true that a composite system is formed by the fusion process but the compound nucleus model can not be employed in the present case since there are not enough collisions in case of light nuclei to justify the assumption of thermal equilibrium as in the compound nucleus model. Any compound nuclear model has two parts: one is the formation cross section and the second is its decay. We are not concerned about decay but about its formation for which we are using the present model which can tackle fusion at energies far below Coulomb barrier. The pair of convenient parameters, W_r and W_i, have been brought in to link the cross section with the nuclear well, so that it is convenient to describe the phenomenon of resonance and selectivity in damping. The boundary condition for the wave function can be expressed by its logarithmic derivative, which for a square well is given by

$$R\frac{[\sin(Kr)]'}{\sin(Kr)}|_{r=R} = KR\cot(KR) \tag{3.4}$$

and in Coulomb field, it is given by

$$\frac{R}{a_c}\left\{\frac{1}{\chi^2}\cot(\delta_0) + 2\left[\ln\left(\frac{2R}{a_c}\right) + 2A + y(ka_c)\right]\right\} \tag{3.5}$$

so that

$$\begin{aligned}\omega_i &= W_i/\chi^2 = \operatorname{Im}\left[\frac{a_c}{R}(KR)\cot(KR)\right] \\ &= \frac{a_c}{R}\left\{\frac{\gamma_i \sin(2\gamma_r) - \gamma_r \sinh(2\gamma_i)}{2[\sin^2(\gamma_r) + \sinh^2(\gamma_i)]}\right\}\end{aligned} \tag{3.6}$$

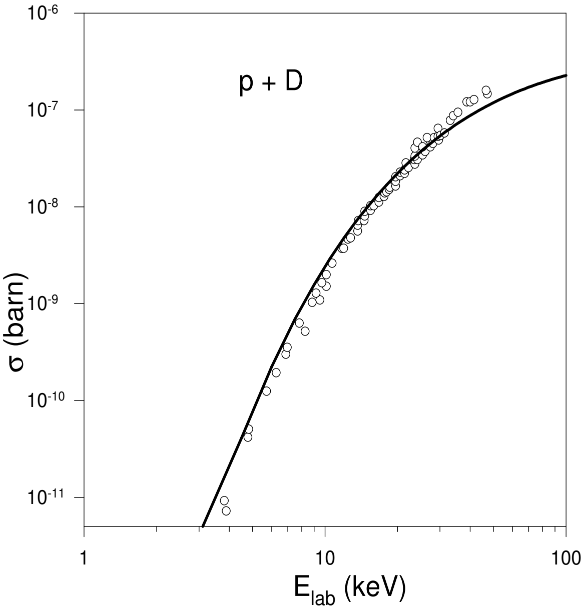

Figure 3.1: Plots of cross section as a function of lab energy for p+D fusion reaction. The continuous line represents the theoretical calculations while the hollow circles represent the experimental data points.

$$\omega_r = W_r/\chi^2 = \frac{a_c}{R}\left\{\frac{\gamma_r \sin(2\gamma_r) + \gamma_i \sinh(2\gamma_i)}{2[\sin^2(\gamma_r) + \sinh^2(\gamma_i)]}\right\} - 2H \tag{3.7}$$

where $K^2 = \frac{2\mu}{\hbar^2}[E - (V_r + iV_i)]$, the real part K_r of K and its imaginary part K_i are related by the equation $K_i = \frac{\mu}{K_r\hbar^2}(-V_i)$, $\gamma = (\gamma_r + i\gamma_i) \equiv (K_rR + iK_iR)$, $H = \left[\ln\left(\frac{2R}{a_c}\right) + 2A + y(ka_c)\right]$, radius of the nuclear well $R = r_0(A_1^{1/3} + A_2^{1/3})$, r_0 is the radius parameter, A_1 and A_2 are the mass numbers of the reacting nuclei, Euler's constant $A = 0.5772156649$ and and $y(ka_c)$ is connected to logarithmic derivative of the Γ function given as $y(x) = \frac{1}{x^2}\sum_{j=1}^{\infty}\frac{1}{j(j^2+x^{-2})} - A + \ln(x)$. In the above relations $k = \sqrt{\frac{2\mu E}{\hbar^2}}$ is the wave number outside the nuclear well.

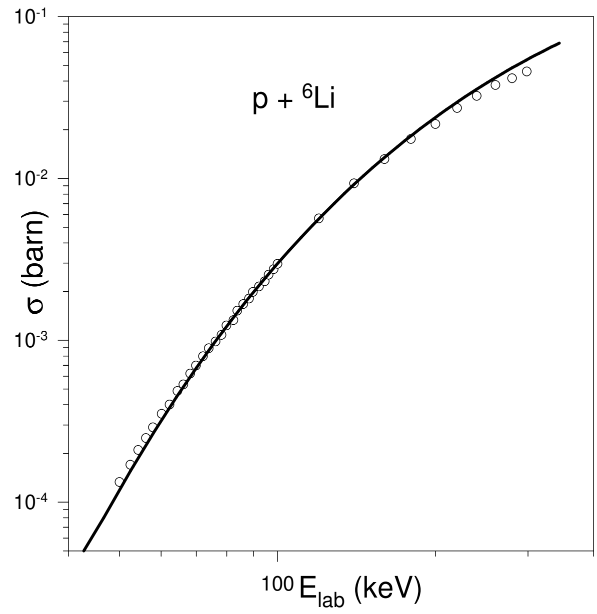

Figure 3.2: Plots of cross section as a function of lab energy for p+^{6}Li fusion reaction. The continuous line represents the theoretical calculations while the hollow circles represent the experimental data points.

3.2 Methodology of theoretical calculations

There are mainly two adjustable parameters, V_r and V_i, in the selective resonant tunnelling model. These are adjusted to meet the resonance peak and the data points covering the entire range of energy. The radius parameter r_0 may be kept fixed or adjusted to fine tune the calculations. In the present calculations, it is varied slightly from one system to the other in order to obtain better theoretical estimates. The fusion cross sections and the dimensionless astrophysical S-functions are calculated using Eq.(3.2) and Eq.(3.3), respectively whereas the astrophysical S-factors (in units of keV-barn) can be calculated using the relation $S(E)=\frac{\pi\hbar^2 \exp(2\pi\eta)}{2\mu\chi^2}S_r(E)$ obtained by comparing Eq.(2.1) with Eq.(3.2).

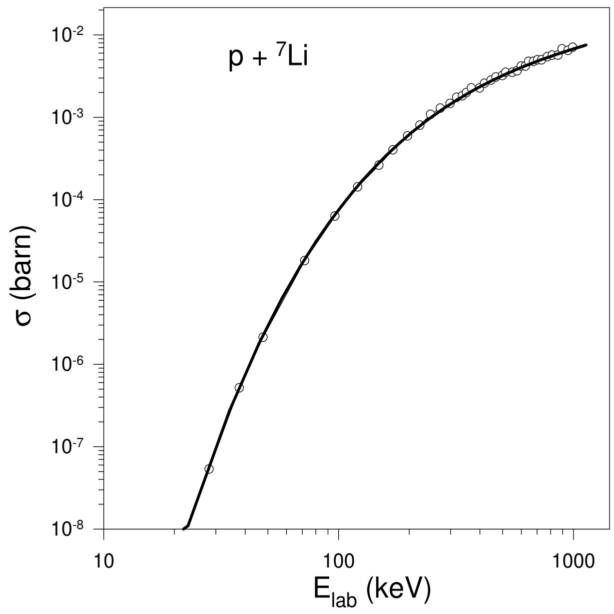

Figure 3.3: Plots of cross section as a function of lab energy for p+^{7}Li fusion reaction. The continuous line represents the theoretical calculations while the hollow circles represent the experimental data points.

3.3 Results and discussion

The present formalism has been used to calculate the fusion cross sections for D+D, D+T, D+^{3}He, p+D, p+^{6}Li and p+^{7}Li. While the first three [50, 51, 52, 53, 54, 55] of these fusion reactions have been done in past with a completely different motive of fusion power production, the rest have been explored in the present work with an intention to use all these six reactions for astrophysical purposes. For reactions D+D, D+T and D+^{3}He, we use the same V_r, V_i and R from Refs. [55], [55] and [53], respectively. For the rest of the fusion reactions, V_r and V_i are adjusted to meet the position and magnitude of the resonance peak in the fusion cross section. The radius parameter r_0 (or equivalently the radius of the nuclear well R defined after Eq.(3.7)) has been further adjusted to fine tune so that the calculations reproduces the experimental data points covering the entire range of energy.

Table 3.1: Values of potential parameters for fusion reactions

Reactions	V_r [MeV]	V_i [keV]	r_0 (fm)
D+D	-48.52	-263.27	2.778
D+T	-40.69	-109.18	1.887
D+^{3}He	-11.859	-259.02	3.331
p+D	-55.0	-0.0235	1.177
p+^{6}Li	-44.25	-7500	1.180
p+^{7}Li	-85.0	-395.0	1.330

The results of present calculations for cross sections of D+D, D+T, D+^{3}He fusion reactions have been shown to compare well [56] with experimental data as well as those calculated using the three and five parameter fitting formulas of Ref.[55]. The results of the cross section calculations for D+D, D+T, D+^{3}He fusion reactions are available in Ref.[55], Ref.[55] and Ref.[53], respectively and the magnitudes of V_r, V_i and r_0 for these three cases are provided in Table-3.1. The large difference in the radius parameter r_0 reflects the fact that nuclear radius of tritium is smallest while that for ^{3}He is largest [57]. The scattering cross section mainly depends on real part of the potential and the radius parameter. Since the scattering cross sections for D+D, D+T, D+^{3}He are of same order, the radius parameter of D+^{3}He being largest, forces the real part of the potential to be smallest.

The results of the cross section calculations for p+D, p+^{6}Li and p+^{7}Li fusion reactions are [58] shown in Figs.-3.1-3.3, and the magnitudes of V_r, V_i and r_0 for these three cases are tabulated in Table-3.1. It is interesting to note that the magnitude of V_i for fusion of p+^{6}Li is about twenty times larger compared to that of p+^{7}Li. The reason may be attributed to extremely low lifetime of ^{8}Be inhibiting its formation. The reason for extremely small V_i in case of p+D system lies in the fact that the binding energy for deuteron is very

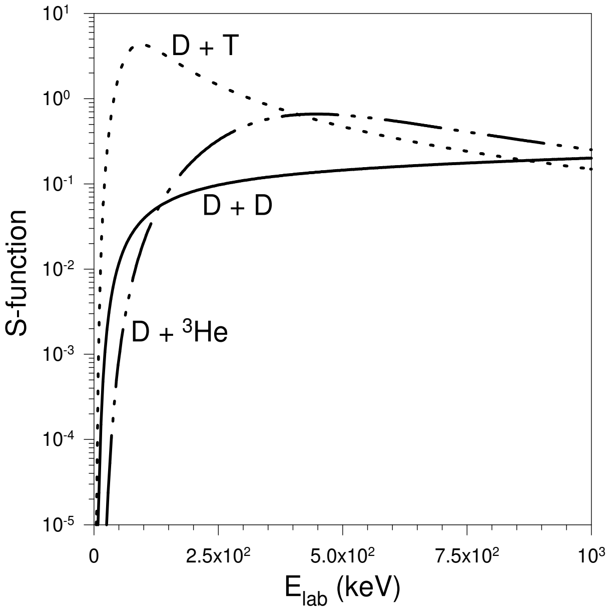

Figure 3.4: Plots of S-function as a function of lab energy for D+D, D+T, D+^{3}He fusion reactions.

small and therefore it easily disintegrates into p+n causing very small p+D fusion cross section and correspondingly very small V_i. The experimental data [59] and the quantum-mechanical calculations show very good agreement [12]. In similar works, new three parameter formula describes well the low energy behavior of the fusion cross section for light nuclei [60, 61]. The results of present calculations for dimensionless S-functions, given by Eq.(3.5), are shown in Figs.-3.4-3.5. Somewhat, mismatch with experimental data in case of p+D fusion reaction may be due to lack of experimental data points and any conclusion at this stage regarding drawback of resonance tunnelling model in case of heavier nuclei would be improper. However, calculations of fusion cross sections for reactions involving medium and heavy nucleus-nucleus systems do need, altogether, a completely different approach [62].

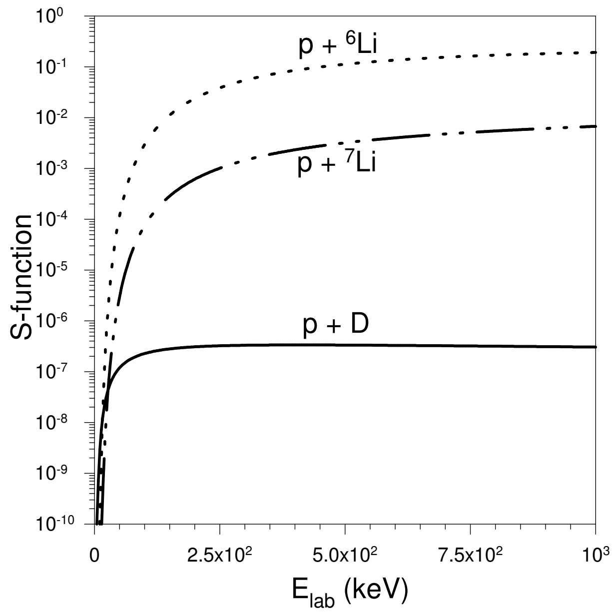

Figure 3.5: Plots of S-function as a function of lab energy for p+^{6}Li, p+^{7}Li and p+D fusion reactions.

3.4 Summary and conclusion

In the deep sub-barrier fusion of light nuclei, the nuclear resonance not just selects the frequency or the energy level only but damping as well that causes reaction between nuclei. When the resonance occurs, the selectivity becomes very sharp. In such selective resonant tunnelling processes the neutron-emission reaction is suppressed. The process of fusion of light nuclei at very low energies can recall the phase factor of the wave function describing the system. The imaginary part in the square well potential describes the formation of compound nucleus [63] formed by the fusion process, but there are not enough collisions to justify the assumptions for compound nucleus model in case of light nuclei. There is no such independent decay process in the light nuclei. In the compound nuclear model, reaction is assumed to proceed in two steps: first fusing to form the compound nucleus followed by its decay. In the present calculations that deal with selective resonant tunnelling, the probability of tunnelling itself depends upon the decay lifetime and is a single step process of fusion of two light nuclei. The agreement with the experimental data for the deep sub-barrier fusion of light nuclei also suggests that such tunnelling proceeds in single step. The recent findings of halo nuclei [64] further strengthens the fact that the nucleons can keep their features without forgetting the memory of wave function while inside the well of the strongly interacting nuclear region. However, the situation is totally different from the astrophysical reactions, since the weakly bound nature is essential in halo nuclei, whereas a low level density plays an important role in astrophysical reactions implying that the mechanism is different between halo nuclei and astrophysical reactions for a nucleus to retain its identity inside the barrier.

The complex potential causes absorption of the projectile into the nuclear well. For over last few decades researches on controlled nuclear fusion have been focused mostly on D-T fusion since it has large fusion cross section compared to that of D-D fusion reaction cross section by a very large factor of the order of several hundred in spite of both having almost the same Coulomb barrier. The reason for a large cross section of the D+T reaction can be attributed to a resonance state near 100 keV. A simple square-well potential model with an imaginary part can be used to describe the D+T nuclear fusion as well as other very light nuclei fusion reactions. The D+D, D+T, D+^{3}He, p+^{6}Li, p+^{7}Li and p+D fusion reactions are of astrophysical importance. It is worthwhile to mention here that the nuclear potential's real part is primarily determined from the resonance energy whereas its imaginary part is obtained by Gamow factor at the resonance energy. The consistency between the present quantum-mechanical calculation and the experimental data suggests strongly of selective resonant tunnelling. The penetrating particle keeps memory of its wave function's phase factor. The applications of the model of the selective resonant tunnelling can be explored further for other fusion reactions among light nuclei.

Chapter 4

ASTROPHYSICAL THERMONUCLEAR REACTION RATES

The astrophysical thermonuclear reactions generate energy that makes stars shine. These are also responsible for the synthesis of the elements in stars. The interstellar medium are enriched with the nuclear ashes when stars eject part of their matter through various means. These processes provide the building blocks for the birth of new stars, of planets and of life itself. The theory of production of elements is called nucleosynthesis and in describing the nuclear processes in stars that are located so far away from us in space and time, it is remarkably successful. The process of synthesis of the elements can be broadly classified into two categories: the primordial or big-bang nucleosynthesis and the steller nucleosynthesis. As the name suggests the primordial nucleosynthesis refers to what happened at the beginning of the universe when light elements such as D, T, ^{3,4}He, ^{6,7}Li and ^{7}Be were synthesized while steller nucleosynthesis occurs in stars and causes synthesis of heavier elements. It is also worthy of attention how the theory predicts these processes based on the quantum mechanical properties of atomic nuclei. The nuclear energy generation in stars, nucleosynthesis and other issues at the intersection of astrophysics and nuclear physics make up the science of nuclear astrophysics. Similar to most areas of physics, it involves both experimental and theoretical activities. In the following these concepts with special emphasis on nuclear processes and their interplay in stars will be described.

4.1 Thermonuclear Cross Sections

The cross section for nuclear interaction (scattering or reaction) can be defined as

$$\sigma = \frac{\text{No. of interactions/time/target nucleus}}{\text{No. of incident particles/time/area}} \tag{4.1}$$

and hence it has the dimension of area. It follows from the definition that

$$\frac{\text{No. of reactions}}{\text{s}} = \frac{\text{No. of incident particles}}{\text{s}} \times \frac{\text{No. of target nuclei}}{\text{Area}} \times \sigma \tag{4.2}$$

The above relation can be written as

$$r = r_{ij} = n_i n_j v_{ij} \sigma \tag{4.3}$$

where σ is the reaction cross section, $r = r_{ij}$ is the no. of reactions/volume/s, n_j is the no. of target nuclei/volume, v_i is the velocity of incident particle, v_j is the velocity of target nuclei and $\vec{v}_{ij} = |\vec{v}_i - \vec{v}_j|$ is the relative velocity.

4.1.1 Nuclear Astrophysical Plasmas: Ion Distribution Functions

Under astrophysical conditions, interacting nuclei in plasma are in thermal equilibrium at temperature T and the individual particles follow a distribution of velocities. It is assumed that the plasma is non-degenerate and non-relativistic and the temperatures being high it is assumed to follow the Maxwell-Boltzmann velocity [65, 66, 67] distribution. The number of reactions per unit volume per unit time r_{ij} should, therefore, be rewritten as

$$r_{ij} = \frac{1}{1+\delta_{ij}} \int \int \sigma |\vec{v}_i - \vec{v}_j| d^3 n_i d^3 n_j \tag{4.4}$$

where Kronecker delta δ_{ij} prevents double counting in the case of identical particles and

$$\begin{aligned} d^3 n_i &= n_i \Big[\frac{m_i}{2\pi kT}\Big]^{3/2} \exp\Big(-\frac{m_i v_i^2}{2kT}\Big) d^3 v_i = n_i \phi(v_i) d^3 v_i \\ d^3 n_j &= n_j \Big[\frac{m_j}{2\pi kT}\Big]^{3/2} \exp\Big(-\frac{m_j v_j^2}{2kT}\Big) d^3 v_j = n_j \phi(v_j) d^3 v_j \end{aligned} \tag{4.5}$$

Here $d^3 n_i$ and $d^3 n_j$ are the number of particles per unit volume having velocities between v_i & $v_i + dv_i$ and v_j & $v_j + dv_j$ respectively.

4.1.2 Thermonuclear Reaction Rates

Thus reaction rate per unit volume, r_{ij} can be written as $r_{ij} = \frac{n_i n_j}{1+\delta_{ij}} < \sigma v >$, where n_i, n_j are the number of particles of type i, j per unit volume with any velocity. Therefore, reaction rate per pair of particles (i, j) is given by

$$< \sigma v > = \int_0^\infty \int_0^\infty \phi(v_i)\phi(v_j) \sigma v_{ij} d^3 v_i d^3 v_j \tag{4.6}$$

The variables v_i and v_j are related to the variables $v = v_{ij}$, the relative velocity and V, velocity of the center of mass , by the usual kinematic relations $v = |\vec{v}_i - \vec{v}_j|$ and

$V = |\frac{m_i\vec{v}_i+m_j\vec{v}_j}{m_i+m_j}|$. Using the reduced mass $\mu = \frac{m_i m_j}{m_i+m_j}$ and the total mass $M = m_i + m_j$, the rate $< \sigma v >$ can be written as

$$< \sigma v >= \int_0^\infty \int_0^\infty \phi(V)\phi(v)\sigma(v)v \; d^3V \; d^3v \tag{4.7}$$

where the transformed velocity distribution $\phi(V)$ and $\phi(v)$ are :

$$\begin{aligned} \phi(V)d^3V = & \quad 4\pi V^2\Big[\frac{M}{2\pi kT}\Big]^{3/2} \exp\Big(-\frac{MV^2}{2kT}\Big)dV \\ \phi(v)d^3v = & \quad 4\pi v^2\Big[\frac{\mu}{2\pi kT}\Big]^{3/2} \exp\Big(-\frac{\mu v^2}{2kT}\Big)dv \end{aligned} \tag{4.8}$$

These are Maxwell-Boltzmann distribution with usual normalization and hence $\int_0^\infty \phi(v)d^3v = \int_0^\infty \phi(V)d^3V = 1$ and

$$< \sigma v >= 4\pi\Big[\frac{\mu}{2\pi kT}\Big]^{3/2} \int_0^\infty v^3\sigma(v)\exp\Big(-\frac{\mu v^2}{2kT}\Big) \; dv \tag{4.9}$$

Using the energy in centre-of-mass frame $E = \frac{1}{2}\mu v^2$, the above equation can be written in the form

$$\begin{aligned} < \sigma v >= & \quad 4\pi\Big[\frac{\mu}{2\pi kT}\Big]^{3/2} \int_0^\infty \Big(\frac{2E}{\mu}\Big)^{3/2}\sigma(v)\exp\Big(-\frac{E}{kT}\Big)\frac{1}{2}\Big(\frac{2}{\mu}\Big)^{1/2}E^{-1/2}dE \\ = & \quad 4\pi\Big[\frac{\mu}{2\pi kT}\Big]^{3/2} \int_0^\infty \sigma(E)\exp\Big(-\frac{E}{kT}\Big)\frac{1}{2}\Big(\frac{2}{\mu}\Big)^{2}E \; dE \\ \Rightarrow \quad < \sigma v >= & \quad \Big[\frac{8}{\pi\mu}\Big]^{1/2}\Big[\frac{1}{kT}\Big]^{3/2} \int_0^\infty \sigma(E)\exp\Big(-\frac{E}{kT}\Big)E \; dE \end{aligned} \tag{4.10}$$

In case of one of the particles being photon $i \equiv \gamma$ and using $h\nu = E_\gamma$ & Planck's distribution for photons

$$\begin{aligned} d^3n_i = & \quad d^3n_\gamma = \Big[\frac{8\pi\nu^2}{c^3}\Big]\frac{d\nu}{\exp(\frac{h\nu}{kT})-1} = \frac{8\pi E_\gamma^2 dE_\gamma}{c^3h^3[\exp(\frac{E_\gamma}{kT})-1]} \\ \Rightarrow \quad d^3n_\gamma = & \quad \frac{1}{\pi^2(\hbar c)^3}\frac{E_\gamma^2}{\exp(\frac{E_\gamma}{kT})-1}dE_\gamma \end{aligned} \tag{4.11}$$

and v_{ij} is always equal to the velocity of light c and hence

$$\begin{aligned} \gamma = & \quad \frac{1}{\pi^2(\hbar c)^3}\int d^3n_j \int_0^\infty \frac{c\ \sigma(E_\gamma)E_\gamma^2}{\exp(\frac{E_\gamma}{kT})-1}dE_\gamma \qquad (4.12) \\ \text{where} \quad \int d^3n_j = & \quad \int n_j\phi(v_j)\ d^3v_j = n_j\int \phi(v_j)\ d^3v_j = n_j \cdot 1 = n_j \\ \text{and hence} \quad \lambda_j = & \quad \frac{r}{n_j} = \frac{1}{\pi^2(\hbar c)^3}\int_0^\infty \frac{c\ \sigma(E_\gamma)E_\gamma^2}{\exp(\frac{E_\gamma}{kT})-1}dE_\gamma \end{aligned}$$

where the symbol λ_j is used in case of one of the interacting particle being γ, instead of $< \sigma v >$ which is used for particle-particle interaction.

4.2 Analytical Parametrization of Reaction Rates

The reaction rates used in BBN reaction network have temperature dependence. Although there are many neutron induced reactions which also have temperature dependence, but few like ^{6}Li(n,γ)^{7}Li are constant with respect to temperature. This has drawn our attention. At thermal energies neutron absorption cross section shows an approximate $1/v$ behavior. Hence, using $\sigma(E) \propto E^{-1/2}$ in Eq.(4.10) immediately shows that the reaction rates are approximately constant with respect to temperature at low energies. However, this fact is true for thermal neutrons ($\sim$ 0.025 eV) only with energies of the order of eV and below. But at energies of astrophysical interest, the neutron induced reaction cross sections can be given by $\sigma(E) = \frac{R(E)}{v}$ [15], where $R(E)$ is a slowly varying function of energy [27] and is similar to the astrophysical S-factor and one expects $\langle\sigma v\rangle$ to be dependent on temperature.

The computer code TALYS [68] allows a comprehensive astrophysical reaction rate calculations apart from other nuclear physics calculations. To a good approximation, in the interior of stars the assumption of a thermodynamic equilibrium holds and nuclei exist both in the ground and excited states. This assumption along with cross sections calculated from compound nucleus model for various excited states facilitates Maxwellian-averaged reaction rates. For stellar evolution models this is quite an important input. The nuclear reaction rates are generally evaluated using the statistical model [69, 70] and astrophysical calculations mostly use these reaction rates. Stellar reaction rate calculations have been routinely done in past [71, 72]. However, TALYS has extended these calculation by adding some new and important features. Apart from coherent inclusion of fission channel it also includes reaction mechanism that occurs before equilibrium is reached, multi-particle emission, competition among all open channels, width fluctuation corrections in detail, coupled channel description in case of deformed nuclei and level densities that are parity-dependent. The nuclear models are also normalized for available experimental data using separate approaches such as on photo-absorption data the E1 resonance strength or on s-wave spacings the level densities .

In the low energy domain, compound nucleus is formed by the fusion of the projectile and the target nuclei. While the total energy E^{tot} is fixed from energy conservation, the total spin J and parity Π can have a range of values. The reaction obeys the following conservation laws,

$$\begin{aligned}
E_a + S_a &= E_{a'} + E_x + S_{a'} = E^{tot}, \quad \text{energy conservation,} \\
s + I + l &= s' + I' + l' = J, \quad \text{angular momentum conservation,} \\
\pi_0 \Pi_0 (-1)^l &= \pi_f \Pi_f (-1)^{l'} = \Pi, \quad \text{parity conservation.}
\end{aligned}$$

The formula for binary cross section, assuming the compound nucleus model, is given by

$$\begin{aligned}
\sigma_{\alpha\alpha'}^{comp} &= D^{comp} \frac{\pi}{k^2} \sum_{J=mod(I+s,1)}^{l_{\max}+I+s} \sum_{\Pi=-1}^{1} \frac{2J+1}{(2I+1)(2s+1)} \sum_{j=|J-I|}^{J+I} \sum_{l=|j-s|}^{j+s} \sum_{j'=|J-I'|}^{J+I'} \sum_{l'=|j'-s'|}^{j'+s'} \qquad (4.13) \\
& \times \delta_\pi(\alpha) \delta_\pi(\alpha') \frac{T_{\alpha lj}^J(E_a) \langle T_{\alpha' l' j'}^J(E_{a'}) \rangle}{\sum_{\alpha'', l'', j''} \delta_\pi(\alpha'') \langle T_{\alpha'' l'' j''}^J(E_{a''}) \rangle} W_{\alpha lj\alpha' l' j'}^J,
\end{aligned}$$

The glossary of symbols used in the equations mentioned above are:

E_a = the energy of the projectile

l = the orbital angular momentum of the projectile

s = the spin of the projectile

j = the total angular momentum of the projectile

π_0 = the parity of the projectile

$$\delta_\pi(\alpha) = \begin{cases} 1 & \text{if } (-1)^l \pi_0 \Pi_0 = \Pi \\ 0 & \text{otherwise} \end{cases}$$

α = the designation of the channel for the initial projectile-target system:

$\alpha = \{a,\ s,\ E_a,\ E_x^0,\ I,\ \Pi_0\}$, where a and E_x^0 are the type of the projectile and the excitation energy (which is zero usually) of the target nucleus, respectively

$l_{\max}$ = the maximum l-value of the projectile

S_a = the separation energy

$E_{a'}$ = the energy of the ejectile

l' = the orbital angular momentum of the ejectile

s' = the spin of the ejectile

j' = the total angular momentum of the ejectile

π_f = the parity of the ejectile

$$\delta_\pi(\alpha') = \begin{cases} 1 & \text{if } (-1)^{l'} \pi_f \Pi_f = \Pi \\ 0 & \text{otherwise} \end{cases}$$

α' = the designation of channel for the ejectile-residual nucleus final system:

$\alpha' = \{a',\ s',\ E_{a'},\ E_x,\ I',\ \Pi_f\}$, where a' and E_x are the type of the ejectile and the residual nucleus excitation energy, respectively

I = the spin of target nucleus

Π_0 = the parity of target nucleus

I' = the spin of residual nucleus

Π_f = the parity of residual nucleus

J = the total angular momentum of the compound system

Π = the parity of the compound system

D^{comp} = the depletion factor so as to take into account for pre-equilibrium and direct effects

k = the wave number of the relative motion

T = the transmission coefficient

W = the correction factor for width fluctuation (WFC).

The velocities of both the targets and projectiles obey Maxwell- Boltzmann distributions corresponding to ionic plasma temperature T at the site. The astrophysical nuclear reaction rate can be calculated by folding the Maxwell-Boltzmann energy distribution for energies E at the given temperature T with the cross section given by Eq.(4.13). Additionally, target nuclei exist both in ground and excited states. The relative populations of various energy states of nuclei with excitation energies E_x^μ and spins I^μ in thermodynamic equilibrium follows the Maxwell-Boltzmann distribution. In order to distinguish between different excited states the superscript μ is used along with the incident α channel in the formulas that follow. Taking due account of various target nuclei excited state contributions, the effective nuclear reaction rate in the entrance channel $\alpha \to \alpha'$ can be finally expressed as

$$N_A\langle\sigma v\rangle^*_{\alpha\alpha'}(T) = \left(\frac{8}{\pi m}\right)^{1/2}\frac{N_A}{(kT)^{3/2}G(T)}\int_0^\infty \sum_\mu \frac{(2I^\mu+1)}{(2I^0+1)} \times \tag{4.14}$$
$$\sigma^\mu_{\alpha\alpha'}(E)E\exp\left(-\frac{E+E_x^\mu}{kT}\right)dE,$$

where N_A is the Avogadro number which is equal to 6.023×10^{23}, k and m are the Boltzmann constant and the reduced mass in the α channel, respectively, and

$$G(T) = \sum_{\mu} (2I^{\mu} + 1)/(2I^0 + 1) \exp(-E_x^{\mu}/kT)$$

is the temperature dependent normalized partition function. By making use of the reciprocity theorem, the reverse reaction cross sections or rates can also be estimated.

Table 4.1: Reaction Rate in units of cm^{3}s^{-1}mol^{-1} for the reaction ^{6}Li(n,γ)^{7}Li as a function of temperature T_9 (expressed in units of 10^9 K) generated from TALYS [68].

T_9	Reaction Rate	T_9	Reaction Rate	T_9	Reaction Rate
0.0001	408.43	0.3	436.44	2.5	824.89
0.0005	440.24	0.4	466.02	3.0	883.00
0.001	423.09	0.5	492.41	3.5	936.22
0.005	414.78	0.6	516.58	4.0	985.55
0.01	392.78	0.7	539.18	5.0	1074.75
0.05	369.81	0.8	560.55	6.0	1153.17
0.1	375.42	0.9	580.88	7.0	1222.50
0.15	388.01	1.0	600.31	8.0	1284.74
0.2	403.71	1.5	686.76	9.0	1342.36
0.25	420.29	2.0	760.28	10.0	1397.99

The reaction rate for the reaction ^{6}Li(n,γ)^{7}Li has been calculated theoretically using the TALYS [68] code. Although, in this reaction the nuclei involved are light, the results of the calculations may be reasonable since apart from the compound nuclear contribution, it accounts for the pre-equilibrium and the direct effects as well. The result of the calculation for reaction rate in units of cm^{3}s^{-1}mol^{-1} as a function of temperature T_9 (expressed in units of 10^9 K) generated from TALYS [68] code is presented in Table-4.1.

In order to provide analytical parametrization of reaction rate for neutron capture reactions [73], the results presented in Table-4.1 has been fitted quite accurately as a

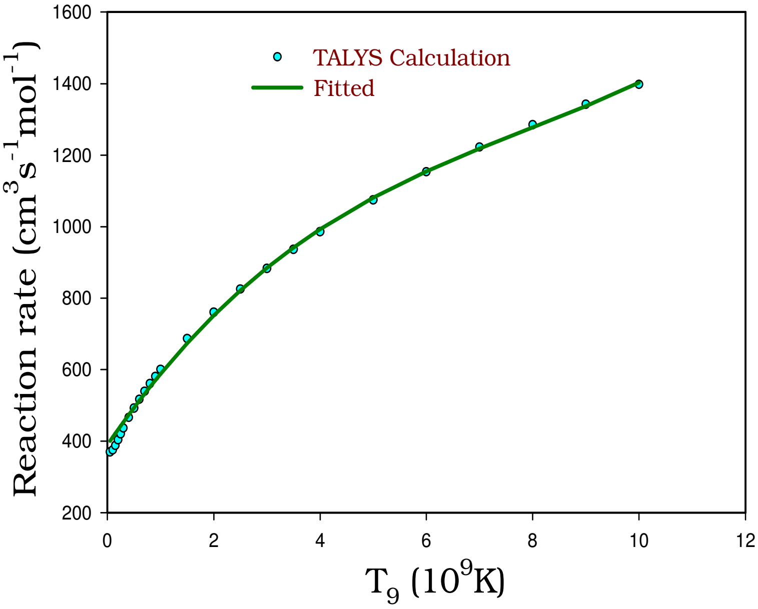

Figure 4.1: Plot of reaction rate as function of temperature T_9. The dots represent results of calculations using TALYS [68] while the continuous line represents the fit to it.

function of T_9. The plot of reaction rate as a function of temperature T_9 is shown in Fig.-4.1. The dots represent results of calculations using TALYS [68] while the continuous line represents its fitting by the function of T_9: $389.5+218.1T_9-20.21T_9^2+0.853T_9^3$. This yields a new reaction rate equation given by $N_A <\sigma v>= 389.5 + 218.1T_9 - 20.21T_9^2 + 0.853T_9^3$ cm^{3}s^{-1}mol^{-1}. This reaction rate is meant to supersede the earlier reaction rate used in the BBN calculations.

4.3 Theoretical Calculations and Results

All the reaction rates used in BBN reaction network have temperature dependence except few neutron induced reactions like ^{6}Li(n,γ)^{7}Li. The Malaney-Fowler reaction rate [74] for ^{6}Li(n,γ)^{7}Li in the BBN reaction network calculations has been taken as 5.10$\times$10^3 cm^{3}s^{-1}mol^{-1} which is constant with respect to temperature. Since this reaction rate is independent of temperature and remained so for several decades, it attracted special attention for further investigation of its temperature dependence. A new reaction rate equation has been developed as a function of T_9 (in units of 10^9 K) by fitting the results for this reaction rate generated from TALYS [68] which turns out to be $N_A < \sigma v >= 389.5 + 218.1T_9 - 20.21T_9^2 + 0.853T_9^3$ cm^{3}s^{-1}mol^{-1}. The results for elemental abundances remained unchanged whether Malaney-Fowler reaction rate or this new reaction rate or any other reaction rate [75] is used for it. However, this new reaction rate may find its usefulness in other domains of nuclear astrophysics.

Chapter 5

BIG-BANG NUCLEOSYNTHESIS

The Hubble expansion of the Universe, the Cosmic Microwave Background Radiation (CMBR) and the big bang nucleosynthesis (BBN) are the three signatures of the big bang model. These are supported by a large number of observational evidences. The BBN, which predicts the primordial abundances of the light elements such as D, ^{3,4}He and ^{6,7}Li, whose syntheses took place few seconds after the big-bang [76] and then the rapidly evolving universe allowed only the nucleosynthesis of the lightest nuclei. In addition to the stable nuclei D, ^{3,4}He and ^{6,7}Li, during the BBN some unstable radioactive isotopes like ^{3}H and ^{7,8}Be were also synthesized. These unstable isotopes ultimately became stable isotopes by either fusing with other nuclei or by decaying. From the beginning of space expansion, BBN lasted during the period from three to about twenty minutes and thereafter, the density and temperature of the universe fell below the threshold required for nuclear fusion reaction to take place and hence averted elements heavier than beryllium to be synthesized primordially and simultaneously it did allow unburned light elements (that did not undergo fusion), such as deuterium, to still exist.

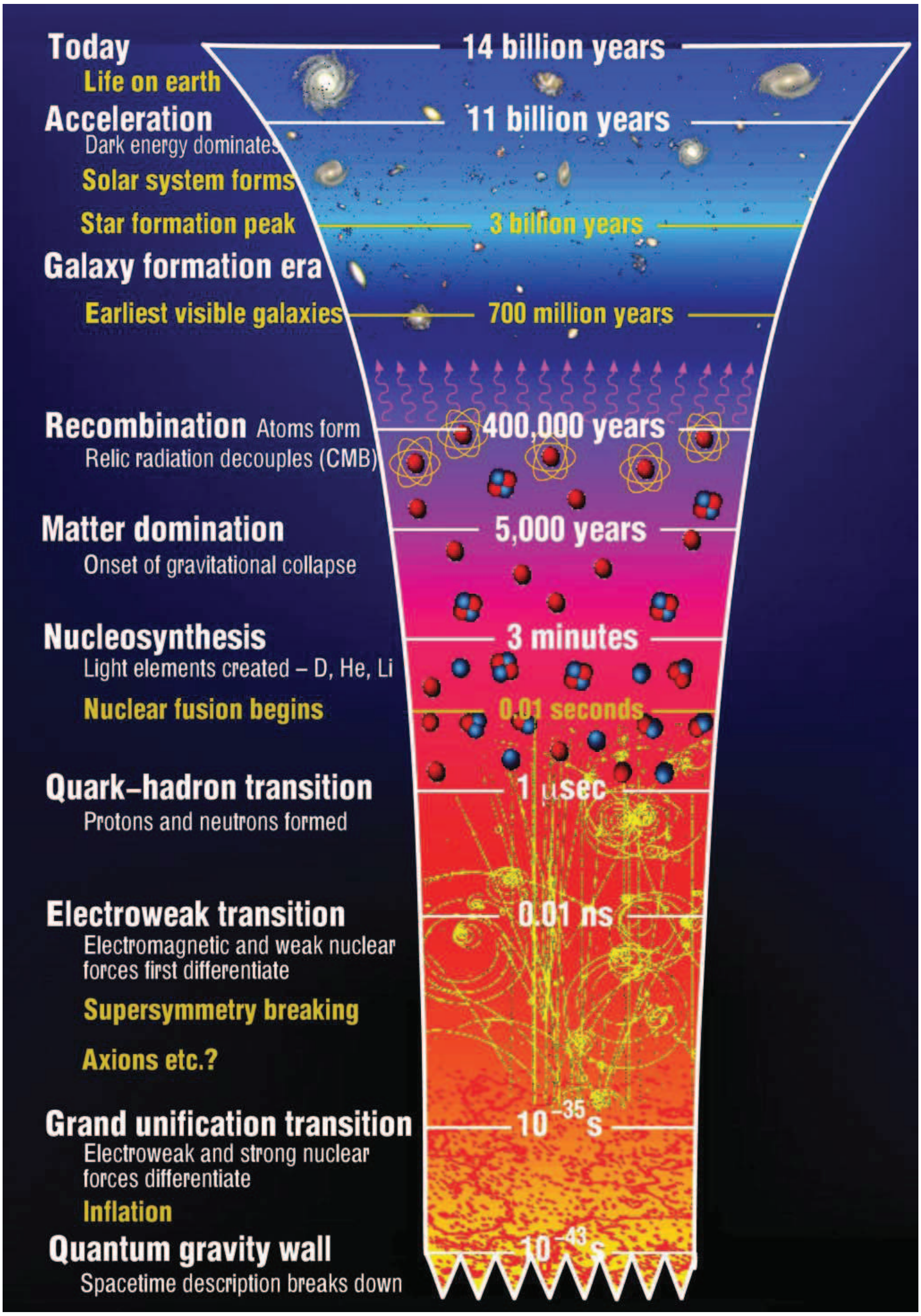

Figure 5.1: The history of our Universe. The vertical time axis is not linear in order to show early events on a reasonable scale. (Photo Courtesy: www.ctc.cam.ac.uk)

5.1 Time Evolution of the Early Universe

The nucleosynthesis calculation requires the knowledge of the temperature and the time evolution of baryonic density. These can be calculated from the thermodynamic considerations and the expansion rate of the universe. The Friedmann-Robertson-Walker (FRW) metric given by

$$ds^2 = dt^2 - a^2(t)\Big(\frac{dr^2}{1-kr^2} + r^2(d\theta^2 + sin\theta d\phi^2)\Big) \tag{5.1}$$

describes the geometry of the universe which assumes homogeneity and isotropy, where the scale factor $a(t)$ describes the expansion and k = 0, ± 1 denotes the flat, closed or open universe, respectively. From Einstein equations one obtains

$$H^2(t) = \Big(\frac{\dot{a}}{a}\Big)^2 = \frac{8\pi G(\rho_R + \rho_M)}{3} - \frac{k}{a^2} + \frac{\Lambda}{3} \tag{5.2}$$

where $H(t)$ is the Hubble parameter, G is the gravitational constant, ρ_M and ρ_R are the matter and radiation densities respectively and Λ is the cosmological constant. It is convenient to consider the critical density $\rho_C = \frac{3H_0^2}{8\pi G}$ for a flat (Euclidean) space corresponding to $k = 0$, $\Lambda = 0$ in Eq.(5.2) for the density components of universe.

As is well known, during the early stages of expansion the matter density (dark and baryonic) $\rho_M \propto a^{-3}$, while the radiation density $\rho_R \propto a^{-4}$. During the BBN epoch, when a is about 10^{-8} times the present value, $H(t)$ is controlled solely by relativistic particles whereas there is no role of the cosmological constant, curvature terms and the matter density. In this case Eq.(5.2) takes the form

$$\Big(\frac{\dot{a}}{a}\Big)^2 = \frac{8\pi G}{3} a_R \frac{g_*(T)}{2} \times T^4 \tag{5.3}$$

where the Stefan-Boltzmann law $a_R T^4$ for the radiation energy density is used and g_* is the effective spin factor which reduces as and when the temperature falls below a threshold mass for the annihilation of every species of particle with its antiparticle. During BBN, only electron and positron annihilates implying that the photons, neutrino/anti-neutrino and e^+/e^- contribute to $g_*(T)$ before they annihilate. The energy released gets shared by those particles which were in equilibrium with baryons and photons but not neutrinos because it occurs after they decouple. Using the constraint that the entropy densities of neutrinos and photons+electrons stay separately constant during the adiabatic expansion [77, 78] and by solving Eq.(5.3) [79, 80] numerically, the neutrino temperature, the photon/ion temperature and the baryonic density can be obtained as a function of time. These are the important inputs required for BBN calculations along with the thermonuclear reaction rates. The expansion rate of the universe remains unaffected by the baryonic density at this epoch. However, the higher baryonic density causes larger number of nuclear reactions per unit time, thereby influencing nucleosynthesis.

Standard BBN theory predictions depend upon the astrophysical nuclear reaction rates and on three more parameters, namely, the number of light neutrino flavours (N_ν), the neutron lifetime (τ_n) and the baryon-to-photon ratio ($\eta_{00} = n_B/n_\gamma$) in the universe [81, 82]. In its standard $N_\nu = 3.0$ form, BBN is a parameter-free theory because of the precise knowledge of the baryon-to-photon ratio of the Universe from the observations of the anisotropies of the CMBR. The big-bang cosmology relies on the Hubble expansion, CMBR and the BBN. The primordial nucleosynthesis or the BBN traces back to the beginning of the universe and deals with nuclear physics, particle physics and cosmology. In spite of the fact that the Hubble expansion may also be explained by using other theories of cosmology, the evidences of CMBR and the observations of the BBN implies a universe which was extremely dense and hot at the very beginning. As described above, the standard scenario for the BBN theory is the FRW cosmological model. The facts that the solution to Einstein equations leads to a homogeneous and isotropic universe implying uniformity of the CMBR temperature across the sky, which is $T = 2.7277 \pm 0.002$

K, and the successfulness of the standard BBN theory validate this approximation. The Friedmann equation relates the big-bang expansion rate, H, to the thermal properties of the particles present at that epoch. The strong interaction in nuclear reactions produces complex nuclei whereas the weak interaction transforms neutrons into protons and *vice versa*. The rates of these processes are involved during expansion. The syntheses of light elements in the early universe is ascertained by the time during its expansion.

5.2 The BBN reaction network

The reactions which took place during BBN can be organized into two categories, *viz* the nuclear reactions which convert neutrons to protons and *vice versa*: n $\leftrightarrow$ p + e^- + $\bar{\nu}_e$; n + e^+ $\leftrightarrow$ p + $\bar{\nu}_e$ and p + e^- $\leftrightarrow$ n + ν_e and the rest of the other reactions. The first categorization is in terms of the mean lifetime of neutrons while the second categorization is on the basis of cross section measurements of different nuclear reactions. The deuterium formation starts with the p + n $\leftrightarrow$ D + γ process. This is an exothermic reaction releasing 2.2246 MeV of energy. The photons are 10^9 times more numerous than protons, therefore photo-destruction rate is more than the production rate of deuterons. Hence the deuterium formation reaction can proceed only when the temperature drops to about 0.3 MeV by the expanding universe. The reactions that make ^{4}He nuclei: D $+ n \rightarrow$ ^{3}H $+ \gamma$, ^{3}H + p $\rightarrow$ ^{4}He + γ, D + p $\rightarrow$ ^{3}He + γ, ^{3}He + n $\rightarrow$ ^{4}He + γ follow once the deuteron formation starts. Apart from the ^{4}He (normal helium), ^{3}He (light helium) is also formed along with the ^{3}H. The ^{4}He nucleus has a binding energy of 28.3 MeV and is more bound than the deuterons. Moreover, the temperature of the plasma by this time has dropped down to 0.1 MeV already, forces these reactions (being photo-reactions) to proceed one way only. The reactions: D + D $\rightarrow$ ^{3}He + n, D + D $\rightarrow$ ^{3}H + p, ^{3}He + D $\rightarrow$ ^{4}He + p, ^{3}H + D $\rightarrow$ ^{4}He + n also produce ^{3}He and ^{4}He. These four reactions are not associated with the relatively slow process of emission of photons and hence usually proceed faster. The reaction between deuterons and other charged particles eventually stops due to electrostatic repulsion when the temperature falls too low to overcome it. When these reactions stops, the ratio of deuteron to proton is very small as it varies as -1.6 power of the total density of neutrons and protons. Most of the neutrons of the universe at that epoch end up as ^{4}He nuclei. At the time of deuteron formation, neutron:proton ratio is about 1:7 and 25% of the mass ends up in the synthesis of the helium. After about 100 seconds of the big-bang the deuterium concentration peaks which subsequently ends up in helium nuclei. Thereafter, a very small amount of helium nuclei can fuse to form heavier nuclei producing a small BBN ^{7}Li abundance. As half-life of ^{3}H which decays into ^{3}He is twelve years, so no primordial ^{3}H can survive till now. Similarly, half-life of ^{7}Be which decays into ^{7}Li is fiftythree days, so no primordial ^{7}Be also can exist today.

Instead of cross sections σ, the thermonuclear reaction rates are used as the inputs to BBN calculations. These rates are calculated by folding Maxwell-Boltzmann energy distribution with energy dependent nuclear reaction cross sections. Thus the Maxwellian-averaged reaction rate per interacting particle pair $< \sigma v >$ at a temperature T, can be described by the equation [8, 28] given below:

$$< \sigma v >= \Big[\frac{8}{\pi\mu(k_B T)^3}\Big]^{1/2} \int \sigma(E) E \exp(-E/k_B T) dE, \tag{5.4}$$

where k_B, E, μ and v are, respectively, the Boltzmann constant, the energy in centre-of-mass frame, the reduced mass of the reactants and the relative velocity. At energies much below the Coulomb barrier, the radius of the nucleus is too small compared to the classical turning point. In this situation $\exp(-2\pi\eta)$ approximates the tunnelling probability through the barrier quite well, where $\eta = \frac{Z_1 Z_2 e^2}{\hbar v}$ is the Sommerfeld parameter with Z_1 and Z_2 being the atomic numbers of the interacting nuclei and e being the elementary charge. As a consequence, the charge induced cross section is factorized as

$$\sigma(E) = \frac{S(E)\exp(-2\pi\eta)}{E} \tag{5.5}$$

where $S(E)$ being the astrophysical S-factor is a smooth function of energy (insofar the narrow resonances are excluded) and hence facilitating extrapolation of the experimentally measured cross sections down to the energies of astrophysical regime. For the narrow resonance case, in general a Breit-Wigner expression approximates the resonant cross section, whereas at low energies the cross sections for neutron induced reaction is given by $\sigma(E) = \frac{R(E)}{v}$ [15] with $R(E)$ being a function which changes slowly with energy [27] and is similar to S-factor.

BBN Network Diagram

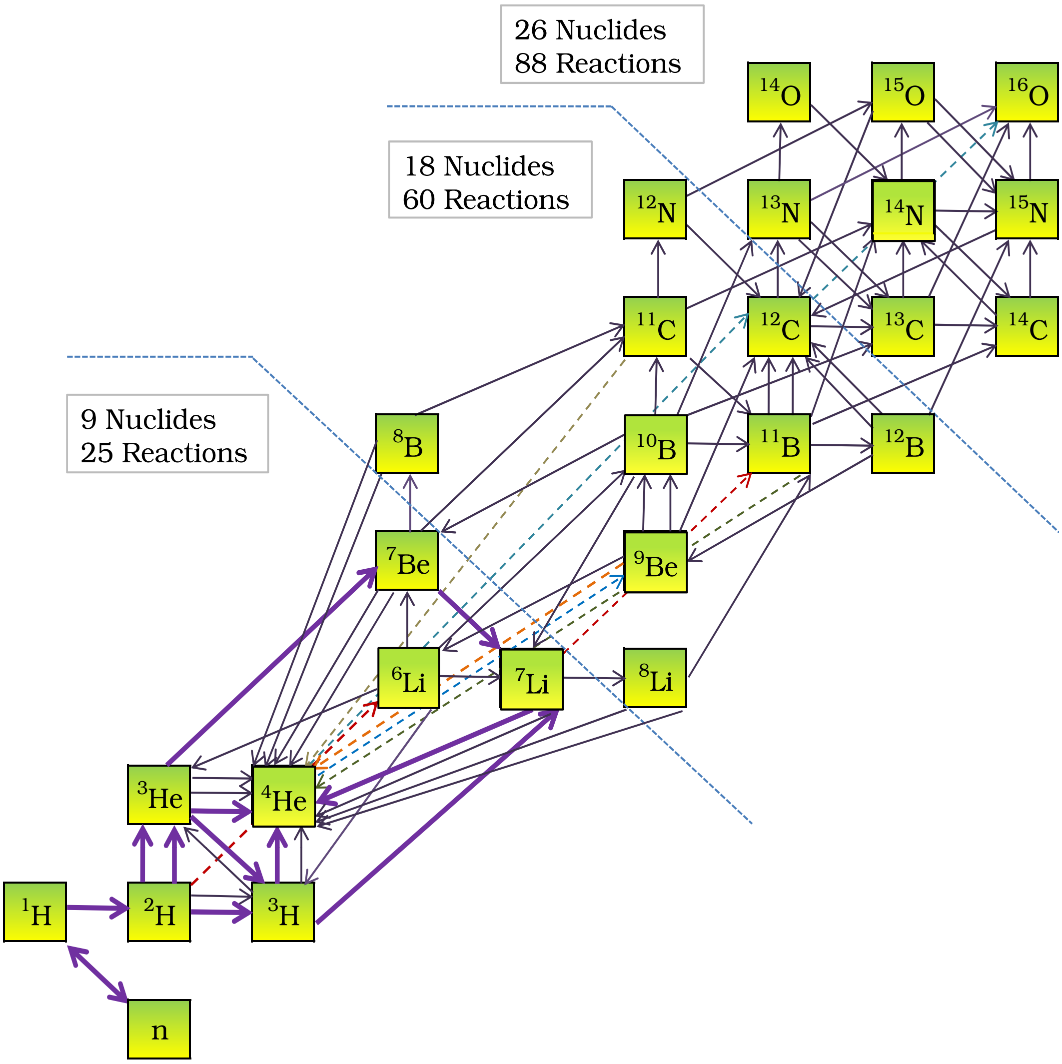

Figure 5.2: Plot of the Nuclear Reaction Network used for Big Bang Nucleosynthesis. The twelve most important reactions have bold arrows.

Chapter 6

PRIMORDIAL ABUNDANCES OF ELEMENTS

Although, there is a good match between primordial abundances of D and ^{3,4}He deduced from observations and from primordial nucleosynthesis calculations, but that of ^{6,7}Li are off by quite large factors. The standard BBN theory predictions depend upon the astrophysical nuclear reaction rates and additionally on three more parameters, *viz.*, the number of light neutrino flavours, the neutron lifetime and the baryon-to-photon ratio in the Universe. The observations by the Wilkinson Microwave Anisotropy Probe [WMAP] [83, 84] and the Planck [85, 86] space missions enabled precise extraction of the baryon-to-photon ratio of the Universe. The standard theory of the weak interaction provides for the weak reaction rates involved in n-p equilibrium. These rates are obtained [87] using neutron lifetime as the only experimental input, whose recent experimental value, 880.3$\pm$1.1 s [88], may be further updated [89, 90], that influence the production of ^{4}He [91]. In the past, sensitivity of the predictions to various parameters and physics inputs in the BBN model were investigated [92, 93, 94, 95, 96, 97, 98].

The cardinal inputs for modeling the stellar evolution and BBN are the nuclear reaction rates per particle pair $< \sigma v >$ in the BBN and stellar network calculations, where σ and v are, respectively, the reaction cross section for nuclear fusion and the relative velocity between the interacting nuclei. These low energy fusion cross sections σ, some of which are not sufficiently well known, can be obtained from laboratory experiments [92, 93, 94, 95, 96]. However, for a given temperature T, a Maxwellian velocity distribution describes v well. The cross section measurements are influenced by various factors involved whereas the theoretical thermonuclear reaction rate estimates depend upon the several approximations taken into consideration. In the network calculations, the Maxwellian-averaged thermonuclear reaction rates needs to be taken into account and the variations [99, 100] in these thermonuclear reaction rates have an effect on the predictions of elemental abundances in stellar evolution and the BBN.

In the present work, we have taken into account the effects of the thermonuclear reaction rates, neutron lifetime and the baryon-to-photon ratio on the primordial abundances of elements. The effect of the modification of thirty-five thermonuclear reaction rates on the abundance of light elements in BBN was investigated earlier. We have used the most recent values of neutron lifetime and baryon-to-photon ratio and further modified reaction rates for d(^{4}He,γ)^{6}Li, t(^{4}He,γ)^{7}Li and ^{3}He(^{4}He,γ)^{7}Be, which is used directly for estimating the formation of ^{7}Li as a result of β^+ decay, by the most recent rate equations in the temperature ranges up to $5T_9$ (in units of 10^9 K) [101, 102, 103, 104, 105]. We have studied abundance yields of light element as functions of temperature and evolution time.

6.1 Observed Primordial Abundances

After BBN, ^{4}He is synthesized in stars as well whose primordial abundance can be deduced from the observations of the ionized hydrogen regions of compact blue galaxies. Galaxies are considered as more primitive since these are formed by the agglomeration of dwarf galaxies, in a hierarchical structure formation paradigm. To take into account the stellar production of ^{4}He, the observations are extrapolated to zero, followed by atomic physics corrections. Aver et al. [106] have obtained its mass fraction to be 0.2449 ± 0.0040.

Deuterium can be destroyed after BBN throughout stellar evolution. Its primordial abundance is estimated from the observations of cosmological clouds in the line of sight of highly redshifted distant quasars. Recently, Cooke et al. [107] have reanalyzed existing data as well as made new observations that led to D/H relative abundance of $(2.53 \pm 0.04) \times 10^{-5}$ with lesser uncertainties than earlier estimates.

Contrary to ^{4}He, ^{3}He is not only produced but also destroyed in stars resulting in its abundance to be not well known as a function of time. Because of the observational difficulties of helium and the small ^{3}He/^{4}He ratio, ^{3}He has only been observed in our Galaxy and its relative abundance is estimated to be $(1.1 \pm 0.2) \times 10^{-5}$ [108].

The BBN started approximately three minutes from the beginning of space expansion and continued for about next seventeen minutes. Consequently, the density and the temperature of the expanding universe dropped to a value which prevented syntheses of elements heavier than beryllium, while enabling unburned light elements (which did not undergo fusion), such as deuterium, to exist at the same time. The heavier element nucleosynthesis takes place mainly in massive stars. During the evolution of galaxies, these stars explode as supernovae and eject heavy element enriched matter into the interstellar medium. Accordingly, the abundances of heavier elements increase with time in stars. Therefore, the abundance of metals (elements heavier than ^{3,4}He) observed is an indication of its age. To be explicit, those having the lower metallicity are the older ones. Hence, observations from the objects having very small metallicity are the candidates for extracting primordial abundances. After BBN ^{7}Li can both be produced (AGB stars, novae, spallation) and destroyed (in the stellar interiors). In the halo of our Galaxy, very old stars are still observable since the life span of lower than one solar mass stars is greater than the age of our universe. At the surface of these stars ^{6,7}Li can be observed. Its abundances were found to be remarkably constant with respect to metallicity as long as it is below the metallicity of the Sun ($\approx$0.1). This constant plateau [109] of Lithium abundance has been correlated to the production of ^{7}Li during BBN. Therefore, it should reflect the primordial value since thinness of the plateau implies that the surface Lithium depletion probably has not been very effective. Sbordone's et al. [110] analysis provides $^{7}\mathrm{Li/H} = (1.58^{+0.35}_{-0.28}) \times 10^{-10}$.

6.2 Calculations of Abundances in Primordial Nucleosynthesis

In a previous work [111], thirty-five Maxwellian-averaged thermonuclear reaction rates from Caughlan et al. [99] and Smith et al. [112] used in the Kawano/Wagoner BBN code [77, 79, 80] were modified by using the latest compilations of Angulo et al. [100] and Descouvemont et al. [73] and its effects were studied with regard to the elemental abundances in primordial nucleosynthesis. These reactions were d(p,γ)^{3}He, d(d,n)^{3}He, d(d,p)t, d(α,γ)^{6}Li, t(d,n)^{4}He, t(α,γ)^{7}Li, ^{3}He(n,p)t, ^{3}He(d,p)^{4}He, ^{3}He(^{3}He,2p)^{4}He, ^{3}He(α,γ)^{7}Be, ^{4}He(αn,γ)^{9}Be, ^{4}He($\alpha\alpha,\gamma$)^{12}C, ^{6}Li(p,γ)^{7}Be, ^{6}Li(p,α)^{3}He, ^{7}Li(p,α)^{4}He, ^{7}Li(α,γ)^{11}B, ^{7}Be(n,p)^{7}Li, ^{7}Be(p,γ)^{8}B, ^{7}Be(α,γ)^{11}C, ^{9}Be(p,γ)^{10}B, ^{9}Be(p,dα)^{4}He, ^{9}Be(p,α)^{6}Li, ^{9}Be(α,n)^{12}C, ^{10}B(p,γ)^{11}C, ^{10}B(p,α)^{7}Be, ^{11}B(p,γ)^{12}C, ^{11}B(p,$\alpha\alpha$)^{4}He, ^{12}C(p,γ)^{13}N, ^{12}C(α,γ)^{16}O, ^{13}C(p,γ)^{14}N, ^{13}C(α,n)^{16}O, ^{13}N(p,γ)^{14}O, ^{14}N(p,γ)^{15}O, ^{15}N(p,γ)^{16}O and ^{15}N(p,α)^{12}C [111]. In the present work we have employed the most recent values of neutron lifetime and the baryon-to-photon ratio and further modified ^{3}He(^{4}He,γ)^{7}Be reaction rate which is used directly for estimating the formation of ^{7}Li as a result of β^{+} decay [102, 104]. We have also used the most recent parametrization for t(^{4}He,γ)^{7}Li and d(^{4}He,γ)^{6}Li reaction rates in the temperature ranges up to $5T_9$ [102, 104], though it is found that these two modifications produced little effect on ^{7}Li abundance over the earlier ones. We have also compared results of the present calculations with our previous one [111] and other recent calculations [113, 114, 115], the most recent one [115] used the same values of τ_n and η_{00} as our present work and performed calculations based on the PARTHENOPE code.

6.2.1 Impact of fundamental constants on the primordial nucleosynthesis

Apart from the astrophysical nuclear reaction rates, the primordial abundances depend upon three more parameters, the number of light neutrino flavours, the neutron lifetime and the baryon-to-photon ratio in the universe. In standard form the number of light neutrino flavours N_ν is taken as 3.0. The observations by the WMAP [83, 84] and the Planck [85, 86] space missions enabled precise extraction of the baryon-to-photon ratio of the Universe as $\eta_{00} = 6.0914 \pm 0.0438 \times 10^{-10}$. The most recent experimental value for the neutron lifetime τ_n which is 880.3 ± 1.1 s [88] has been used in the present calculations.

6.2.2 Thermonuclear reaction rates for radiative d^{4}He, t^{4}He and ^{3}He^{4}He captures

The twelve most relevant nuclear reactions that affect most the predictions of elemental abundances of light nuclei [^{4}He, D, ^{3}He, ^{7}Li] are n−decay, p(n,γ)d, d(p,γ)^{3}He, d(d,n)^{3}He, d(d,p)t, ^{3}He(n,p)t, t(d,n)^{4}He, ^{3}He(d,p)^{4}He, ^{3}He(α,γ)^{7}Be, t(α,γ)^{7}Li, ^{7}Be(n,p)^{7}Li and ^{7}Li(p,α)^{4}He. The uncertainties for the reactions ^{3}He + ^{4}He $\rightarrow$ ^{7}Be + γ, ^{3}H + ^{4}He $\rightarrow$ ^{7}Li + γ and p + ^{7}Li $\rightarrow$ ^{4}He + ^{4}He directly reflect uncertainty in the predicted yield of ^{7}Li.

The ^{3}He(^{4}He,γ)^{7}Be reaction rate which is used directly for estimating the formation of

^{7}Li as a result of β^+ decay is now replaced by the most recent rate equation [102, 104]. The refined variant of calculations for the astrophysical S-factor of the d(^{4}He,γ)^{6}Li, t(^{4}He,γ)^{7}Li and ^{3}He(^{4}He,γ)^{7}Be reactions, are in better agreement with the previously available as well as the most recent experimental data and its predictive reliability is also demonstrated. The new parametrization for the reaction rates [102, 104] given, respectively, by

$$\begin{aligned} N_A < \sigma v >= \quad & 17.128/T_9^{2/3} \exp(-7.266/T_9^{1/3}) \\ & \times(1.0 - 4.686\ T_9^{1/3} + 15.877\ T_9^{2/3} \\ & -21.523\ T_9 + 18.703\ T_9^{4/3} - 4.554\ T_9^{5/3}) \\ & +53.817/T_9^{3/2} \exp(-6.933/T_9), \end{aligned} \tag{6.1}$$

$$\begin{aligned} N_A < \sigma v >= \quad & 2304.319/T_9^{2/3} \exp(-6.165/T_9^{1/3}) \\ & \times(1.0 - 25.706\ T_9^{1/3} + 74.057\ T_9^{2/3} \\ & +28.460\ T_9 - 61.303\ T_9^{4/3} + 19.591\ T_9^{5/3}) \\ & +29.322/T_9^{3/2} \exp(-1.641/T_9), \end{aligned} \tag{6.2}$$

$$\begin{aligned} N_A < \sigma v >= \quad & 36807.346/T_9^{2/3} \exp(-11.354/T_9^{1/3}) \\ & \times(1.0 - 15.748\ T_9^{1/3} + 56.148\ T_9^{2/3} \\ & +27.650\ T_9 - 66.643\ T_9^{4/3} + 21.709\ T_9^{5/3}) \\ & +44350.648/T_9^{3/2} \exp(-16.383/T_9) \end{aligned} \tag{6.3}$$

in units of cm^{3}s^{-1}mol^{-1} are used in the temperature ranges up to $5T_9$ for the astrophysical evaluations of ^{6}Li, ^{7}Li and ^{7}Be productions. For temperatures higher than $5T_9$, for d(^{4}He,γ)^{6}Li reaction, Angulo et al. [100] reaction rate has been used. For t(^{4}He,γ)^{7}Li and $^3He(^4He,\gamma)^7Be$ reactions, above $5T_9$ and up to $8T_9$ reaction rates of Descouvemont et al. [73] and above $8T_9$, Angulo et al. [100] reaction rates have been used.

6.3 Results and discussion

An exhaustive study of the effects of fundamental constants and thermonuclear reaction rates on the primordial nucleosynthesis has been carried out. The entire calculations performed so far by us is for the standard Big Bang Nucleosynthesis but with the modified reaction rates [73, 100, 102, 104] and with the most recent experimental value for the neutron lifetime $\tau_n = 880.3 \pm 1.1$ s and with the value of $\eta_{00} = \eta_{10} \times 10^{-10} = 6.0914 \pm 0.0438 \times 10^{-10}$ for the baryon-to-photon ratio. In Table-6.1 the results of present calculations [13, 116] have been compared with the previous one [111] and other recent calculations [113, 114, 115]. The theoretical uncertainties quoted in the table arise out of experimental uncertainties in the magnitudes of τ_n and η_{10}. However, the other dominant source of uncertainty arises from the reaction rates which would certainly increase the theoretical uncertainties quoted in this work.

So far as the accuracy of the calculations is concerned, the computations performed are correct far beyond the results quoted in Table-6.1 where the entries have been rounded up to four significant digits only. Thus the corresponding computational errors are orders of magnitude smaller than those related to the experimental parameters involved. The calculations have been performed using twenty-six nuclides and eighty-eight reaction rates. These include the twelve most important nuclear reactions which are listed in section 6.2.2 and have the largest effects on the predictions of the primordial elemental abundances of light nuclei. Truncation of the reaction network from 26 nuclides and 88 reaction rates to 18 nuclides and 60 reaction rates or to 9 nuclides and 25 reaction rates cause changes in final abundances by only about 0.1% and 0.5%, respectively. Exclusion of reaction rates beyond 88 already included causes no changes so far as the abundances of light elements are concerned.

We find that using the most recent values of fundamental constants and new reaction rate result in marginal decrease in helium mass fraction causing slight improvement than obtained previously in standard BBN calculations. On the contrary, the relative abundances of deuteron and ^{3}He increase marginally, yet remaining within the uncertainties of experimental observations. It is also observed that the yield of ^{7}Li slightly improves ($\sim 12\%$) (which was off by a factor of ~ 3 in the standard BBN calculation) over the standard BBN abundance. It is, therefore, evident that even with appreciable nuclear physics uncertainties, the primordial lithium abundance problem of BBN is hardly influenced by most of these nuclear reaction rates.

Table 6.1: Yields at CMB-WMAP baryonic density ($\eta_{10} = 6.0914 \pm 0.0438$ [83, 84]).

	2012[111]	2014[113]	2015[114]	2016[115]	This work	Observations
^{4}He	0.2479	0.2482±0.0003	0.2484±0.0002	0.2470	0.2467±0.0003	0.2449±0.0040 [106]
D/H ($\times 10^{-5}$)	2.563	$2.64^{+0.08}_{-0.07}$	2.45±0.05	2.579	2.623±0.031	2.53±0.04 [107]
^{3}He/H ($\times 10^{-5}$)	1.058	1.05±0.03	1.07±0.03	0.9996	1.067±0.005	1.1±0.2 [108]
^{7}Li/H ($\times 10^{-10}$)	5.019	$4.94^{+0.40}_{-0.38}$	5.61±0.26	4.648	4.447±0.067	$1.58^{+0.35}_{-0.28}$ [110]

6.4 Summary and conclusion

In summary, the standard BBN theory predictions depend upon the astrophysical nuclear reaction rates and additionally on three more parameters, the number of light neutrino flavours, the neutron lifetime and the baryon-to-photon ratio in the universe. The effect of the modification of thirty-five reaction rates on elemental abundance of light nuclei in BBN was investigated earlier. In the present work we have replaced the neutron lifetime and baryon-to-photon ratio by most recent values and further modified the reaction rates d(^{4}He,γ)^{6}Li, t(^{4}He,γ)^{7}Li and ^{3}He(^{4}He,γ)^{7}Be (which is used directly for estimating the formation of ^{7}Li as a result of β^+ decay) by the most recent equations [102, 104]. We have studied light element abundance yields as functions of the temperature and the evolution time. We found that these changes caused only slight improvement ($\sim 12\%$) on the standard BBN abundance yield of ^{7}Li. In a few other recent studies [113, 114, 115, 117] also it was found that inclusion of some new reaction rates to the BBN code and thus increasing the reaction network had no effect virtually on the BBN abundances. It is interesting to note that the earlier observed relative abundance of ^{7}Li ($1.1 \pm 0.1 \times 10^{-10}$) [118] has been revised upward by $\sim 44\%$ recently [110]. Moreover, if one takes the lower limit of the present theoretical estimate and compares it with the upper limit of the observed value of ^{7}Li relative abundance then these two values appear to be converging but still overestimated by a factor of 2.27. If the other dominant source of uncertainty from the reaction rates is also considered then certainly the theoretical and the observed values would converge further. Nevertheless, the chances of finding solutions by conventional nuclear physics means, to either of the 'lithium problems' are improbable and, if ^{6,7}Li problems remain up to experimental observations in future, we may be compelled to consider more exotic scenarios.

Beyond Standard Model extension of BBN is motivated by the fact that it could find a solution to the lithium abundance problem and test fundamental physics as well as probe the early universe. The expansion rate of the universe may be affected if gravity differs from its general relativistic description and the variation of the fundamental constants may have to be constrained by BBN [119, 120]. The ^{7}Li abundance may be lowered by a massive particle decay during BBN or afterwards. Similar effects with negatively charged relic particles, like the supersymmetric partner of the τ lepton could also be obtained, that could form bound states with nuclei and lower the Coulomb barrier causing enhancement of nuclear reactions [121]. Other nonstandard solutions to the ^{6,7}Li problems comprise of photon cooling [122], possibly combining magnetic fields [123] and particle decays.

Chapter 7

CONCLUDING REMARKS

An analytical model based on nuclear reaction theory for non-resonant fusion cross sections near Coulomb barrier has been developed. The astrophysical S-factors involving stable and neutron rich isotopes of C, O, Ne, Mg and Si for fusion reactions have been calculated in the centre of mass energy range of 2-30 MeV. The present formalism predicts precisely the suppression of S-factor at sub-barrier energies which are of astrophysical interest. The cross sections can be convoluted with Maxwell-Boltzmann distribution of energies to obtain thermo- or pycno- nuclear reaction rates relevant to nucleosynthesis at high density environments and stellar burning at high temperatures as well as for ^{34}Ne + ^{34}Ne fusion occurring in the inner crust of accreting neutron stars.

The present theoretical model is based on the tunnelling through barrier arising out of nuclear, Coulomb and centrifugal potentials. The potential barrier due to nuclear and Coulomb interactions has been assumed to be of parabolic nature. The effect of the centrifugal barrier for $l > 0$ which in turn means the contributions from higher l values have been simulated phenomenologically. Except for this, the entire formulation is exact and does not invoke any other approximation. Compared to the earlier works [10, 44, 43], the present endeavor causes two fold simplifications. This model uses five parameters as against seven parameters used earlier [43] and relies on exact theoretical expressions for barrier penetration rather than the approximated ones [43, 44]. The energy dependence of the astrophysical S-factors for the fusion reactions involving stable and several neutron rich isotopes of C, O, Ne, Mg and Si covering a wide range of energy from 2 MeV to 30 MeV, below and above the Coulomb barrier, have been calculated. The mentioned reactions are merely a few illustrative examples, but the elegance of the theoretical model in describing the experimental data suggests that it may be used successfully for a large number of other nuclei and their isotopes for which a few experimental data covering a reasonable span of energy is available. As the experimental data is not easily available at relevant energies, the main purpose of this theoretical model is to extrapolate, in a reliable way, the experimental data, where ever available, to the astrophysical relevant energies as well as to extend it to other isotopes.

The model described above, however, does not take into account the resonances in the cross sections which are more prominent in case of the deep sub-barrier fusion of light nuclei. When the resonance occurs, the nuclear resonance not just selects the frequency or the energy level only but the damping as well which causes nuclear reactions. The process of fusion of light nuclei at very low energies can recall the phase factor of the wave function describing the system. A simple square-well potential model with an imaginary part has been used here to describe the nuclear fusion of very light nuclei. The imaginary part in the square well potential describes the formation of compound nucleus formed by the fusion process, but there are not enough collisions to justify the assumptions for compound nucleus model in case of light nuclei. There is no such independent decay process in the light nuclei. In the compound nuclear model, reaction is assumed to proceed in two steps: first fusing to form the compound nucleus followed by its decay. In the present calculations that deal with selective resonant tunnelling, the probability of tunnelling itself depends upon the decay lifetime and is a single step process of fusion of two light nuclei. The agreement with the experimental data for the deep sub-barrier fusion of light nuclei also suggests that the tunnelling proceeds in a single step.

This simple model has been used to describe the nuclear fusion of D+D, D+T, D+^{3}He, p+^{6}Li, p+^{7}Li and p+D fusion reactions which are of astrophysical importance. It is important to note that the nuclear potential's real part is primarily determined from the resonance energy while its imaginary part can be obtained by Gamow factor at the resonance energy. The consistency between the present quantum-mechanical calculations performed and the experimental data suggests strongly of selective resonant tunnelling. The potential parameters have been extracted and the radius parameters obtained truly reflects the measured nuclear radii. This model of selective resonant tunnelling model can be applied further to explore for nuclear fusion reactions among other light nuclei.

The primordial elemental abundance predictions of the BBN is one of the three strong evidences for the Big-Bang model apart from the Cosmic Microwave Background and the observational verification of Hubble's expansion. Precise knowledge of the baryon-to-photon ratio of the Universe from observations of the anisotropies of cosmic microwave background radiation has made the Standard BBN a parameter-free theory. Although, there is a good agreement between abundances calculated in primordial nucleosynthesis and those of light elements deduced from observations over nine orders of magnitude, the discrepancy of ^{7}Li abundance higher by a factor of ~ 3 still remains when calculated theoretically. The primordial abundances depend on the astrophysical nuclear reaction rates and on three additional parameters, the number of light neutrino flavours, the neutron lifetime and the baryon-to-photon ratio in the universe. The effect of the modification of thirty-five reaction rates on the elemental abundances in BBN was investigated earlier by us. In the present work we have incorporated the most recent values of neutron lifetime and the baryon-to-photon ratio and further modified ^{3}He(^{4}He,γ)^{7}Be reaction rate which is used directly for estimating the formation of ^{7}Li as a result of β^+ decay as well as the reaction rates for $t(^4He,\gamma)^7Li$ and $d(^4He,\gamma)^6Li$. We find that these modifications reduce the theoretically calculated abundance of ^7Li by $\sim 12\%$.

The Malaney-Fowler reaction rate [74] for $^6Li(n,\gamma)^7Li$ in the BBN reaction network calculations has been taken as 5.10×10^3 $cm^3s^{-1}mol^{-1}$ which is constant with respect to temperature. A new reaction rate equation has been developed as a function of T_9 by fitting the results for this reaction rate generated from TALYS [68]. The results for elemental abundances remained unchanged whether Malaney-Fowler reaction rate or the new reaction rate or any other reaction rate [75] is used for it. However, this new reaction rate may find its usefulness in other domains of nuclear astrophysics. In fact, it has been found that the twelve major BBN reactions *viz.* ^4He, D, ^3He, ^7Li] are n$-$decay, $p(n,\gamma)d$, $d(p,\gamma)^3He$, $d(d,n)^3He$, $d(d,p)t$, $^3He(n,p)t$, $t(d,n)^4He$, $^3He(d,p)^4He$, $^3He(\alpha,\gamma)^7Be$, $t(\alpha,\gamma)^7Li$, $^7Be(n,p)^7Li$ and $^7Li(p,\alpha)^4He$ affect the elemental abundance predictions of light nuclei, the most. To elaborate it further, truncation of the reaction network from 26 nuclides and 88 reaction rates to 9 nuclides and 25 reaction rates cause changes in final abundances by about 0.5% while for 18 nuclides and 60 reaction rates the change is only about 0.1%. Inclusion of reaction rates beyond the 88 reactions which have been included in the present calculations causes minimal changes so far as the abundances of light elements are concerned. In a few other recent studies [113, 114, 115, 117] also it was found that some new reaction rate inclusions in the BBN code and thus increasing the reaction network had no effect virtually on the BBN abundances. Recently the reaction cross section for $^7Be(n,p)^7Li$ reaction, which belongs to the twelve most important reactions affecting abundances, has been measured at CERN [124]. In the region of BBN domain, the new result yields only very minor improvement on the cosmological lithium problem.

It is interesting to note that the earlier observed relative abundance of ^7Li $(1.1\pm0.1\times 10^{-10})$ [118] has been revised upward by $\sim 44\%$ recently [110]. Moreover, if one takes the lower limit of our theoretical estimate and compares it with the upper limit of the observed value of ^{7}Li relative abundance then these two values appear to be converging but still overestimated by a factor of 2.27. If the other dominant source of uncertainty from the reaction rates is also considered then certainly the theoretical and the observed values would converge further. Nevertheless, the chances of finding solutions by conventional nuclear physics means, to either of the 'lithium problems' are improbable and, if ^{6,7}Li problems remain up to experimental observations in future, we may be compelled to consider more exotic scenarios.

Beyond the Standard Model extension to BBN could be used to find a solution to the lithium problem as well as to probe the early universe and test fundamental physics. The rate of expansion of the universe may be affected if gravity differs from its general relativistic description and the variation of the fundamental constants may have to be constrained by BBN [119, 120]. The ^{7}Li abundance may be lowered by a massive particle decay during BBN or afterwards. With negatively charged relic particles, like the supersymmetric partner of the τ lepton, that could form bound states with nuclei and lower the Coulomb barrier leading to the enhancement of nuclear reactions [121]. Other nonstandard answers to the ^{6,7}Li problems comprise of photon cooling [122], possibly combining magnetic fields [123] and particle decay. The possibility of solving either of the unresolved ^{6,7}Li problems by other means, moving to the physics beyond the Standard Model [125] that includes the shortcomings of the Standard BBN model of physics including dark matter, dark energy, matter-antimatter symmetry, gravity such as f(R) gravity generalization of Einstein's general relativity, may be needed to be explored.

Appendix I

Derivation of $\int_{r_1}^{r_2}\sqrt{\frac{V(r)}{E}-1}\ dr$:

At the turning point as shown in Fig.-1.3, $r_1 = a$ and $r_2 = b$. As the inner turning point $r_1 = a$ is extremely small in comparison to b, we can therefore take an approximation, $r_1 = a \to 0$. So,

$$\begin{aligned}
\int_{r_1}^{r_2}\sqrt{\frac{V(r)}{E}-1}\ dr = & \int_{a}^{b}\sqrt{\frac{V(r)}{E}-1}\ dr \\
= & \int_{0}^{b}\sqrt{\frac{V(r)}{E}-1}\ dr \\
= & \int_{0}^{b}\sqrt{\frac{(Z_1Z_2e^2)/r}{E}-1}\ dr \\
= & \int_{0}^{b}\sqrt{\frac{b}{r}-1}\ dr
\end{aligned} \tag{8.1}$$

where we have used $V(r) = (Z_1Z_2e^2)/r$ and $b = \frac{Z_1Z_2e^2}{E}$.

$$\begin{aligned}
\text{Let}\ \ r = b\sin^2\theta \quad & \Rightarrow dr = && 2b\sin\theta\cos\theta d\theta \\
& \Rightarrow dr = && b\sin^2\theta d\theta \\
& \text{Also, as} && r \to 0, \qquad \theta \to 0
\end{aligned}$$

$$
\begin{aligned}
\text{and} \qquad & r \to b, \qquad\qquad \sin^2\theta \to 1 \qquad \Rightarrow \theta \to \pi/2 \\
\text{therefore} \int_0^b \sqrt{\frac{b}{r} - 1}\; dr = \qquad & \int_0^{\pi/2} \sqrt{\text{cosec}^2\theta - 1}\; (2b\sin\theta\cos\theta)\; d\theta \\
= \qquad & \int_0^{\pi/2} \cot\theta\; 2b\sin\theta\cos\theta\; d\theta \\
= \qquad & 2b\int_0^{\pi/2} \cos^2\theta\; d\theta \\
= \qquad & b\frac{\pi}{2} \qquad\qquad (8.2)
\end{aligned}
$$

Bibliography

[1] A. Friedman, Zeitschrift für Physik. **10**, 377 (1922).

[2] Abbé G. Lemaître, Annals of the Scientific Society of Brussels, **47A**, 41 (1927).

[3] Edwin Hubble, Proceedings of the National Academy of Sciences of the United States of America **15**, 168 (1929).

[4] Abbé G. Lemaître, Nature **128**, 704 (1931).

[5] Abbé G. Lemaître, MNRAS **91**, 483 (1931).

[6] Hans A. Bethe, Rev. Mod. Phys. **71**, S6 (1999).

[7] G. Gamow, *Structure of Atomic Nuclei and Nuclear Transformations* (Oxford University Press, 1937).

[8] R. N. Boyd, *An Introduction to Nuclear Astrophysics* (University of Chicago, Chicago, 2008), 1st ed.

[9] D. G. Yakovlev, L. R. Gasques, M. Beard, M. Wiescher and A. V. Afanasjev, Phys. Rev. **C 74**, 035803 (2006).

[10] M. Beard, A. V. Afanasjev, L. C. Chamon, L. R. Gasques, M. Wiescher and D. G. Yakovlev, At. Data Nucl. Data Tables **96**, 541 (2010).

[11] Vinay Singh, Joydev Lahiri and D. N. Basu, Nucl. Phys. **A 987**, 260 (2019).

[12] Vinay Singh, Debasis Atta, Md. A. Khan and D. N. Basu, Nucl. Phys. **A 986**, 98 (2019).

[13] Vinay Singh, Joydev Lahiri, Debasis Bhowmick and D. N. Basu, Journal of Experimental and Theoretical Physics, **155**, 832 (2019); **128**, 707 (2019).

[14] J. R. Newton, C. Iliadis, A. E. Champagne, A. Coc, Y. Parpottas and C. Ugalde, Phys. Rev. **C 75**, 045801 (2007).

[15] J. M. Blatt and V. F. Weisskopf, *Theoretical Nuclear Physics* (John Wiley & Sons, New York; Chapman & Hall Limited, London).

[16] E. M. Burbidge, G. R. Burbidge, W. A. Fowler and F. Hoyle, Rev. Mod. Phys. **29**, 547 (1957).

[17] W. A. Fowler and F. Hoyle, Astrophys. J. Suppl. **9**, 201 (1964); Appendix C.

[18] D. D. Clayton, *Principles of Stellar Evolution and Nucleosynthesis* (University of Chicago Press, Chicago, 1983).

[19] J. C. Niemeyer, S. E. Woosley, Astrophys. J. **475**, 740 (1997).

[20] P. Höflich, Nucl. Phys. **A 777**, 579 (2006).

[21] T. Strohmayer, L. Bildsten, in: W.H.G. Lewin, M. Van der Klis (Eds.), *Compact Stellar X-ray Sources*, (Cambridge University Press, Cambridge, London.), 113 (2006).

[22] H. Schatz, L. Bildsten, A. Cumming, Astrophys. J. **583**, L87 (2003).

[23] A. Cumming, J. Macbeth, J.J.M. in t Zand, D. Page, Astrophys. J. **646**, 429 (2006).

[24] S. Gupta, E.F. Brown, H. Schatz, P. Mller, K.-L. Kratz, Astrophys. J. **662**, 1188 (2007).

[25] P. Haensel, J.L. Zdunik, Astron. Astrophys. **229**, 117 (1990).

[26] P. Haensel, J.L. Zdunik, Astron. Astrophys. **404**, L33 (2003).

[27] Tapan Mukhopadhyay, Joydev Lahiri and D. N. Basu, Phys. Rev. **C 82**, 044613 (2010); *ibid* Phys. Rev. **C 83**, 067603 (2011).

[28] E. G. Adelberger et al., Rev. Mod. Phys. **83**, 195 (2011).

[29] J. R. Patterson, H.Winkler and C. S. Zaidins, Astrophys. J. **157**, 367 (1969).

[30] M. G. Mazarakis and W. E. Stephens, Phys. Rev. **C 7**, 1280 (1973).

[31] M. D. High and B. Cujec, Nucl. Phys. **A 282**, 181 (1977).

[32] K. U. Kettner, H. Lorenz-Wirzba and C. Rolfs, Z. Phys. **A 298**, 65 (1980).

[33] H. W. Becker, K. U. Kettner, C. Rolfs and H. P. Trautvetter, Z. Phys. **A 303**, 305 (1981).

[34] K. A. Erb and D. A. Bromley, Phys. Rev. **C 23**, 2781 (1981).

[35] B. Dasmahapatra, B. Cujec and F. Lahlou, Nucl. Phys. **A 384**, 257 (1982).

[36] L. J. Satkowiak, P. A. DeYoung, J. J. Kolata and M. A. Xapsos, Phys. Rev. **C 26**, 2027 (1982).

[37] P. Rosales et al., Rev. Mex. Fís. **49**, 88 (2003).

[38] E. F. Aguilera et al., Phys. Rev. **C 73**, 064601 (2006).

[39] L. Barrón-Palos et al., Nucl. Phys. **A 779**, 318 (2006).

[40] T. Spillane et al., Phys. Rev. Lett. **98**, 122501 (2007).

[41] L. D. Landau and E. M. Lifshitz, *Quantum Mechanics*, Pergamon, Oxford, (1976).

[42] D. N. Basu, vide figure, e-Print arXiv: nucl-th/0204060 (2002).

[43] A. V. Afanasjev, M. Beard, A. I. Chugunov, M. Wiescher and D. G. Yakovlev, Phys. Rev. **C 85**, 054615 (2012).

[44] D. G. Yakovlev, M. Beard, L. R. Gasques and M. Wiescher, Phys. Rev. **C 82**, 044609 (2010).

[45] L. R. Gasques, A. V. Afanasjev, E. F. Aguilera, M. Beard, L. C. Chamon, P. Ring, M. Wiescher and D. G. Yakovlev, Phys. Rev. **C 72**, 025806 (2005).

[46] L. R. Gasques, A. V. Afanasjev, M. Beard, J. Lubian, T. Neff, M. Wiescher and D. G. Yakovlev, Phys. Rev. **C 76**, 045802 (2007).

[47] M. Assunção and P. Descouvemont, Phys. Lett. **B 723**, 355 (2013).

[48] G. Gamow, Phys. Rev. **53**, 595 (1938).

[49] G. Gamow, Zeits. f. Physik. **51**, 204 (1928).

[50] X. Z. Li, Czechoslovak Journal of Physics **49**, 985 (1999).

[51] X. Z. Li, C. X. Li and H. F. Huang, Fusion Technology **36**, 324 (1999).

[52] Xing Zhong Li, Jian Tian, Ming Yuan Mei and Chong Xin Li, Phys. Rev. **C 61**, 024610 (2000).

[53] Xing Z. Li, Bin Liu, Si Chen, Qing M. Wei and Heinrich Hora, Laser and Particle Beams **22**, 469 (2004).

[54] Xing Z. Li, Nucl. Fusion Plasma Phys. **28**, 257 (2008).

[55] Xing Z. Li, Qing M. Wei and Bin Liu, Nucl. Fusion **48**, 125003 (2008).

[56] Vinay Singh, Debasis Atta and Md. A. Khan, Proceedings of the DAE-BRNS Symp. on Nucl. Phys. **61**, 930 (2016).

[57] The NIST Reference on Constants, Units and Uncertainty, URL: https://physics.nist.gov/cgi-bin/cuu/Value?rd#mid.

[58] Vinay Singh, Debasis Atta, Md. A. Khan and D. N. Basu, Proceedings of the DAE-BRNS Symp. on Nucl. Phys. **63**, 768 (2018).

[59] Chadwick M.B. et al. ENDF/B-VII.0: Next generation evaluated nuclear data library for nuclear science and technology Nucl. Data Sheets **107**, 29313060 (2006).

[60] Xing Z. Li, Zhan M. Dong and Chang L. Liang, J. Fusion Energy **31**, 432 (2012).

[61] C. L. Liang, Z. M. Dong and X. Z. Li, Current Science **108**, 519 (2015).

[62] Debasis Atta and D. N. Basu, Phys. Rev. **C 90**, 064622 (2014).

[63] H. Feshbach, *Theoretical Nuclear Physics* (Wiley, New York, 1992), p. 23.

[64] K. Riisager, Rev. Mod. Phys. **66**, 1105 (1994).

[65] Biao Wang, C. A. Bertulani and A. B. Balantekin, Phys. Rev. **C 83**, 018801 (2011).

[66] C. A. Bertulani, J. Fuqua and M. S. Hussein, Astrophys. J. **767**, 67 (2013).

[67] S.Q. Hou, J. J. He, A. Parikh, D. Kahl and C. Bertulani, arXiv:1408.4422.

[68] A.J. Koning, S. Hilaire, and M.C. Duijvestijn. In Proceedings of the International Conference on Nuclear Data for Science and Technology, 22-27 April 2007, Nice, France. 2008. pp. 211-214.Arjan Koning, Stephane Hilaire and Stephane Goriely, **TALYS-1.4** A nuclear reaction program, December 28, (2011).

[69] T. Rauscher, F.-K. Thielemann and K.-L. Kratz, Phys. Rev. **C 56**, 1613 (1997).

[70] T. Rauscher, Phys. Rev. **C 81**, 045807 (2010).

[71] T. Rauscher and F.-K. Thielemann, Atom. Data Nucl. Data Tables **75**, 1 (2000).

[72] T. Rauscher and F.-K. Thielemann, Atom. Data Nucl. Data Tables **79**, 47 (2001).

[73] P. Descouvemont, A. Adahchour, C. Angulo, A. Coc, E. Vangioni-Flam, Atom. Data Nucl. Data Tables **88**, 203 (2004).

[74] R. A. Malaney and W. A. Fowler, Astrophys. J. **345**, L5 (1989).

[75] Su Jun et al., Chinese Phys. Lett. **27**, 052101 (2010).

[76] F. Hoyle and R. J. Tayler, Nature (London) **203**, 1108 (1964).

[77] L. Kawano, FERMILAB Report No. PUB-92/04-A, January 1992 (unpublished).

[78] S. Weinberg, *Cosmology*, Oxford University Press, 2008, ISBN 978-0-19-852682-7.

[79] R. Wagoner, W. A. Fowler, and F. Hoyle, Astrophys. J. **148**, 3 (1967).

[80] R. Wagoner, Astrophys. J. Supp. **18**, 247 (1969).

[81] C. J. Copi, D. N. Schramm and M. S. Turner, Science **267**, 192 (1995).

[82] C. J. Copi, D. N. Schramm and M. S. Turner, Phys. Rev. Lett. **75**, 3981 (1995).

[83] E. Komatsu et al., Astrophys. J. Suppl. **192**, 18 (2011).

[84] G. Hinshaw et al., Astrophys. J. Suppl. **208**, 19 (2013).

[85] P. A. R. Ade et al. (Planck Collaboration XVI), Astron. Astrophys. **571**, A16 (2014).

[86] P. A. R. Ade et al. (Planck Collaboration XIII), Astron. Astrophys. **594**, A13 (2016).

[87] D. Dicus, E. Kolb, A. Gleeson, E. Sudarshan, V. Teplitz and M. Turner, Phys. Rev. D 26 (1982) 2694.

[88] K. A. Olive et al. (Particle Data Group), Chin. Phys. **C 38**, 090001 (2014) URL: http://pdg.lbl.gov.

[89] F. Wietfeldt and G. Greene, Rev. Mod. Phys. **83**, 1173 (2011).

[90] A. R. Young et al., J. Phys. **G 41**, 114007 (2014).

[91] G. J. Mathews, T. Kajino and T. Shima Phys. Rev. **D 71**, 021302(R) (2005).

[92] K. M. Nollett and S. Burles, Phys. Rev. **D 61**, 123505 (2000).

[93] R. H. Cyburt, B. D. Fields, and K. A. Olive, Astropart. Phys. **17**, 87 (2002).

[94] R. H. Cyburt, Phys. Rev. **D 70**, 023505 (2004).

[95] R. H. Cyburt, B. D. Fields and K. Olive, J. Cosm. Astropart. Phys. **11**, 12 (2008).

[96] P. D. Serpico, S. Esposito, F. Iocco, G. Mangano, G. Miele, and O. Pisanti, J. Cosmol. Astropart. Phys. **12**, 010 (2004).

[97] F. Iocco, G. Mangano, G. Miele, O. Pisanti, and P. D. Serpico, Phys. Rep. **472**, 1 (2009).

[98] G. M. Fuller and C. J. Smith, Phys. Rev. **D 82**, 125017 (2010).

[99] G. R. Caughlan and W. A. Fowler, Atom. Data Nucl. Data Tables **40**, 283 (1988).

[100] C. Angulo et al., Nucl. Phys. **A 656**, 3 (1999).

[101] S. B. Dubovichenko, A. V. Dzhazairov-Kakhramanov and N. A. Burkova, Russ. Phys. J. **60**, 935 (2017).

[102] S. B. Dubovichenko, Russ. Phys. J. **60**, 1143 (2017).

[103] S. B. Dubovichenko, A. V. Dzhazairov-Kakhramanov and N. A. Burkova, Indian J. Phys. **93**, 279 (2019).

[104] Sergey Dubovichenko, Albert Dzhazairov-Kakhramanov and Nataliya Burkova, Int. J. Mod. Phys. **E 28**, 1930004 (2019).

[105] S. B. Dubovichenko, A. V. Dzhazairov-Kakhramanov, N. A. Burkova, R. Ya. Kezerashvili, Ch. T. Omarov, A. S. Tkachenko and D. M. Zazulin, Nucl. Phys. **A 987**, 46 (2019).

[106] E. Aver, K. A. Olive and E. D. Skillman, J. Cosmology Astropart. Phys. **07**, 011 (2015).

[107] R. Cooke, M. Pettini, R. A. Jorgenson, M. T. Murphy and C. C. Steidel, Astrophys. J. **781**, 31 (2014).

[108] T. Bania, R. Rood and D. Balser, Nature **415**, 54 (2002).

[109] F. Spite and M. Spite, Astron. Astrophys. **115**, 357 (1982).

[110] L. Sbordone, P. Bonifacio, E. Caffau et al., Astron. Astrophys. **522**, A26 (2010).

[111] Abhishek Mishra and D. N. Basu, Rom. J. Phys. **57**, 1317 (2012).

[112] M. S. Smith, L. H. Kawano and R. A. Malaney, Astrophys. J. Suppl. **85**, 219 (1993).

[113] A. Coc, J.-P. Uzan and E. Vangioni, J. Cosmology Astropart. Phys. **10**, 050 (2014).

[114] A. Coc, P. Petitjean, J.-P. Uzan, E. Vangioni, P. Descouvemont, C. Iliadis and R. Longland, Phys. Rev. **D 92**, 123526 (2015).

[115] R. H. Cyburt, B. D. Fields, K. A. Olive and T.-H. Yeh, Rev. Mod. Phys. **88**, 015004 (2016).

[116] Vinay Singh, Joydev Lahiri, Debasis Bhowmick and D. N. Basu, Proceedings of the DAE-BRNS Symp. on Nucl. Phys. **62**, 702 (2017).

[117] R. N. Boyd, C. R. Brune, G. M. Fuller and C. J. Smith, Phys. Rev. **D 82**, 105005 (2010).

[118] A. Hosford, S. G. Ryan, A. E. Garcia-Perez, J. E. Norris and K. A. Olive, Astron. Astrophys. **493**, 601 (2009).

[119] A. Coc, K. Olive, J.-P. Uzan and E. Vangioni, Phys. Rev. **D 79**, 103512 (2009).

[120] A. Coc, P. Descouvemont, K. Olive, J.P. Uzan and E. Vangioni, Phys. Rev. **D 86**, 043529 (2012).

[121] M. Kusakabe, K. S. Kim, M.-K. Cheoun, T. Kajino and Y. Kino, Phys. Rev. **D 88**, 063514 (2013).

[122] O. Erken, P. Sikivie, H. Tam and Q. Yang, Phys. Rev. **D 85**, 063520 (2012).

[123] D. G. Yamazaki, M. Kusakabe, T. Kajino, G. J. Mathews and M. K. Cheoun, Phys. Rev. **D 90**, 023001 (2014).

[124] L. Damone et al., Phys. Rev. Lett. **121**, 042701 (2018).

[125] Guo-yuan Huang, Tommy Ohlsson and Shun Zhou, Phys. Rev. **D 97**, 075009 (2018).